Journal of Scientific Exploration, Vol. 19, No. 1, pp. 43–89, 2005 0892-3310/05

An Integrated Alternative Conceptual Framework to Heat Engine Earth, Plate Tectonics, and Elastic Rebound

STAVROS T. TASSOS

Institute of Geodynamics, National Observatory of Athens, P.O. Box 200 48, 118 10 Athens, Greece
e-mail: s.tassos@gein.noa.gr and tasschec@panafonet.gr

DAVID J. FORD

2/22 Mitchell St., Townsville, N.Q., Australia, 4810
e-mail: zzzspace@internode.on.net

Abstract—Physical evidence indicates that a thermally driven Earth, plate tectonics, and elastic rebound theory violate fundamental physical principles, and that Earth is a quantified solid body, the size of which possibly increases with time. Earth's core is considered as a low-temperature, high-energy/high-frequency, high-tension material, wherein new elements form, constituting the Excess Mass (EM), which is then added atom-by-atom to the overlying mantle. Iron, with the highest nuclear binding energy of 8.8 MeV, should be the last element to form. Due ultimately to cosmic stretching, the internal pressure gradient is from the center, toward the surface; so EM ascends as solid state ''wedges'', which upon encountering an anisotropic obstacle, then accumulates due to its blockage. Iron ascends in the form of reduced high pressure Fe^{2-}, to a depth of about 700 km. At shallower depths it then releases 4–5 electrons whilst oxidizing and decompressing at reducing confining pressures. Some of the released excess mass electrons travel as free electrons, and thereby cause microcracks to form when the electron concentration exceeds the threshold of $>10^{18}$ electrons/m^2; these microcracks enlarge as their concentration increases and their cumulative internal electron pressure builds up; via this self-repulsive electron pressure a great mass of rock is uplifted over time. Microcracks serve both as resonant cavities for ''old'' metallic bond electrons from $Fe^{2,3+}$ and ''new'' electrons from Fe^{2-}, radiating at the infrared, and as electrical capacitors, producing effective semiconductor behavior. If and when the concentration of electrons in the microcavity and of p-holes at the rock-microcrack interface surpasses the necessary electro-motive force potential, the electrical impedance to electron flow is attrited and dielectric breakdown occurs, i.e., the transient discharging of electrons very rapidly empties the network of cavities, causing an implosive collapse of the regional network of parallel microcavities. This high-energy implosion coerces the otherwise plastic surrounding rocks to respond instantaneously elastically, and an earthquake is thus generated. The same implosion that caused the earthquake can also produce a fault rupture of the rocks if its transient dynamic shock pressure exceeds the rock's bonded strength. The magnitude of an earthquake depends on the size of the active volume of almost concurrently discharging microcavities. Hence, we are referring to an electromagnetic self-organized

criticality, a direct implication of which is the inherent non-predictability of any earthquake's timing or energy release.

Keywords: frictional resistance—Q factor—heat sources—seismic wave velocity—plate tectonics—subduction—non-elastic crust—elastic rebound—faults—earthquakes—clustering—quanta—iron—nuclear binding energy—pressure—electron—discharge—microcrack—resonant cavity—semiconductor—p-type—n-type—capacitor—threshold—electrical resistance—dielectric breakdown—implosion

Introduction

F. T. Freund, in his paper "Rocks that Crack and Spark and Glow: Strange Pre-Earthquake Phenomena" (*JSE,* 17, 37–71), very successfully showed how erroneous results in rock conductivity measurements become part of mainstream science. We think this is a side effect of a wider problem; mainstream science progressively turns into an ideological system of belief in theories, and as such, it tends to ignore the implications of logic and observations, when these contradict their predicated mental abstractions.

In that context, the current mainstream geosciences are fundamentally based upon three such "ideologies": (a) Plate tectonics, (b) a thermally driven convecting interior, i.e., the "heat engine" Earth abstraction, while (c) Earth's interior is treated as an elastic half-space, in which static stress changes along faults produce earthquakes. Unfortunately, heat is also considered as the "driving force" in alternative non-mainstream propositions, and elastic rebound is also being treated as a realistic approach to earthquake generation and their recurrence. Below we will show some of the simple physical reasons why the present geodynamic and geotectonic paradigms are so dramatically wrong, and why continents cannot move like "rafts" on a "sea" of convecting semifluid hot mantle. We will also demonstrate the incompatibility of earthquake mechanics and rupture mechanics requirements.

Finally, we will propose, for your consideration, an integrated alternative conceptual framework, which we think is compatible with what the Earth actually is: a quantified, solid plastic planet, which is possibly expanding. In other words, such a body's interior dynamic processes are overwhelmingly dominated not by comparatively weak classical thermal kinetic processes of bulk rock convection but by the much more energy concentrated and therefore mechanically capable quantified electronic and electromagnetic processes. Such processes are inevitably and predictably always present and active within any solid, even, of course, our Earth.

The Surface Thermal Gradient

Observations at certain points on the Earth's surface, or very close to it, e.g., down mine shafts and from deep continental drilling projects, show that temperature increases by 20° to 30°C per kilometer. If that thermal gradient

continues unchanged down to a depth of 40 km, the temperature would be from 800° to 1200°C, which is around the melting point of all rocks. Similarly, at the mantle-core boundary, at about 2900 km, it would be from 58,000° to 87,000°C. Nobody claims such absurd ambient temperatures exist in Earth's lower crust or mantle. Actually, considering the amount of heat energy conventionally proposed to do the mechanical work, e.g., to motivate the supposed bulk convection of semi-fluid rocks, the thermal gradient and, therefore, the temperatures inside the Earth, should be much greater than is physically reasonable.

In the plate tectonics context, heat loss should have its highest values in mid-ocean ridges, and it will be gradually reduced moving away from the central ridges, reaching its lowest values in trench and trench-arc gap regions, i.e., at depths of the Benioff zone, shallower than ~100 km. But the data (Pollack *et al*., 1993) indicate that the mean heat flow value is about 60–80 $m\mathrm{W.m}^{-2}$ in oceanic or continental sites, independent of and despite idealised plate tectonics expectations. Also, heat flow values below 30 $m\mathrm{W.m}^{-2}$ are actually common in and near mid-ocean ridges, and values above 150 $m\mathrm{W.m}^{-2}$ are paradoxically common in trenches and back-arcs. The most characteristically contrary examples to standard expectations are those of Japan and Fiji-Tonga (Uyeda, 1986), where most of the deepest earthquakes actually occur, and alleged subduction of cold ''lithospheric'' oceanic slab is thought to occur.

Storetvedt (1997) notes: ''the ridge crests show very large scatter in heat flow magnitudes, including some local highs among a population of dominantly anomalously low values...''.

Most of the known ''hot-spots'' with active volcanoes, e.g., the Hawaiian, Alpine, Rocky Mountains, African ''hot spots'', as well as all active volcanoes along the Pacific ''Ring of Fire'', do not coincide with the in-actual-fact much cooler mid-ocean ridges. Furthermore, the close spatial association of volcanoes, positive geoidal and gravity anomalies, and strong intermediate depth and deep earthquake clusters is likewise evident. Smoot (2002) also notices the spatial association of high heat flow values with elevated surface topography and earthquake activity.

Thus, all our observations indicate that regional high heat flow must be a shallow near-surface phenomenon, and the mechanism of heat production must be common, locally controlled, and cannot be sourced, nor supplied by global scale convective transfer.

The Lack of Heat Sources

Table 1 conveys Earth's estimated annual internal energy budget. The total required power is on the order of 10^{15} W ($\sim 3 \times 10^{22}$ J/yr) and corresponds to all energy involved in an 8.9 earthquake. The bulk of the 10^{15} W, ~95.8%, is used to overcome the frictional-electromagnetic forces that keep the atoms of a solid substance in place within it. Heat loss of about 4.1×10^{13} W (1.3×10^{21} J/yr), is a small fraction, about 4.1% of total seismic moment, while the heat used for lava production is only about 0.08% of total energy, and the 5×10^{10} W of

TABLE 1
Earth's Annual Internal Energy Budget

Energy type	Watts	%
Friction	0.95789×10^{15}	95.789
Heat loss	0.04122×10^{15}	4.122
Lava production	0.00084×10^{15}	0.084
Elastic wave energy	0.00005×10^{15}	0.005
Total energy–seismic moment	1.00000×10^{15}	100.000
Radiogenic thermal energy sources	$<0.01800 \times 10^{15}$	<1.800

seismic wave energy released by earthquakes is the infinitesimal 0.005% of total annual energy demanded.

If the Earth were indeed a heat engine, this would require an equivalent heat energy generation process, capable of routinely supplying this total annual observed interior global energy flow. The conventionally suggested heat sources are (1) remnant primordial heat trapped in Earth at the time of the Earth's presently supposed origin, about 4.6 billion years ago, (2) tidal dynamic heating, and (3) decay of radioactive elements.

With regard to the first option, the 2×10^{30} J (Press & Siever, 1978) of the supposed primordial heat could have lasted for only the first 67 million years, given constant expenditure at the present annual global energy dissipation rates.

For the second option, the 10^{12} W of tidal frictional heat induced in rocks by the about 11 cm oscillatory uplift of the mantle due to the moon's gravitational attraction amounts to an almost insignificant 0.1% of the necessary annual heating energy requirement for a thermally driven convective Earth mantle.

Lastly, the third proposed energy source, the primary radioactive isotopic constituents of Earth, such as Uranium (U) 238, Thorium (Th) 232, and Potassium (K) 40, are routinely cited, or rather, assumed within conventional geodynamics literature, as the most probable mantle heating energy source. According to Press and Siever (1978), the concentrations of Th^{232}, U^{238}, and K^{40} in granite are about 13, 4, and 4 ppm, respectively, a total of 21 ppm, while in basalt the total is only 4 ppm, and in peridodite, which is considered to be a typical mantle rock, their total concentration is the very low 0.1 ppm (Table 2).

Obviously, these isotopes are only found within the uppermost level of granitic-continental rocks, making up a minor fraction of Earth's outer-most thin skin, and are effectively absent from all known rocks of direct mantle origin, such as mantle xenoliths. In other words, conventional geodynamic models misguidedly presume radioactive isotopes to be an adequate origin of the observed annual heat-flow rates, from that essentially non-radioactive mantle.

The direct annual heat equivalent of the 21 ppm radiogenic elements in the crust is $\sim$0.03 J/kg/yr, or $\sim 10^{-9}$ W/kg, and of the 0.1 ppm in peridotite, about 3×10^{-12} W/kg. We have no reason to accept a proposition that the concentration, if any, of radiogenic elements in the mantle and core, i.e., in the about 6×10^{24} kg of Earth's mass, is greater than 0.1 ppm. Therefore, the maximum amount of heat

TABLE 2
Earth's Radioactive Elements and Their Power Supply (Press & Siever, 1978)

	Uranium (ppm)	Thorium (ppm)	Potassium (ppm)	Total ppm	Total Watts/kg
Granite	4	13	4	21	10^{-9}
Basalt	0.5	2	1.5	4	1.6×10^{-10}
Peridotite	0.02	0.06	0.02	0.1	3×10^{-12}

all such radiogenic sources could optimally provide is a meagre 1.8×10^{13} W; i.e., less than 1.8% of Earth's observed annual energy usage (Table 1).

Consequently, plate tectonics has no identified energy source, because these three proposed interior heat energy sources are logically assessed to be pathetically inadequate. Also, they are incompatible with the sorts of thermally driven geodynamic processes proposed and envisioned by plate tectonics.

In short, we observe that Earth's upper levels are being continually heated. That anomalous heating strongly associates spatially with earthquakes, crustal uplift, and volcanism; but there is presently no feasible, nor even remotely credible, rationale to account for this observed global heat energy's origins or physical mechanism. Therefore, the conventional Earth's interior energy model must be put aside.

The Diffusion of Thermal Energy

Heat is ''random'' kinetic energy because it refers to the oscillatory vibrational movements of ''free'' particles and/or atomic constituents with random vectors. It is conventionally apparent that the greater the mass and velocity of the particle, the greater the measurable energy equivalent ''heat'' content and measured temperature it will have. In contrast to heat energy, electromagnetic energy is locally ''concentrated'' and has an implicit net polarised ''directionality''. For that reason, its mechanical efficiency is extremely high over short distances, i.e., the concentrated electromagnetic energy dissipative losses due to simple mechanical friction are comparatively minuscule and therefore prohibitive for heating-induced bulk convection.

For example, for an electron to move with a velocity of the order of 10,000 km/s—a velocity which is very common for free electrons, i.e., electrons polarized, concentrated and accelerated within a cathode ray tube—the necessary induced kinetic heating temperature equivalent of that velocity is 2.2 million degrees. If such temperatures had ever existed within Earth's interior, Earth would have exploded to become a tenuous gas 4.6 billion years ago. However, this same electron velocity of 10,000 km/s requires only 285 volts of short-range polarised and directed electromagnetic energy input, or just a little higher than that provided from a typical domestic AC mains supply. It is this type of electromagnetic excitation which we propose to be the far more rational

and probable mechanism of Earth's upper mantle and crust heating and observed geodynamic processes.

The latent heat of melting of basalt is about 2×10^6 J/kg, or ~1.4 km/s speed squared, which corresponds to an acceleration of about 1.4 km/s^2. Since this energy must be readily available the required power must likewise be of the same order, i.e., $\sim 2 \times 10^6$ W/kg. The available power due to radiogenic sources in the crust is the infinitesimal $\sim 10^{-9}$ W/kg, and in the mantle the even lower $\sim 3 \times 10^{-12}$ W/kg. In practical terms, this means that in order for upper mantle and/or crust partial melting to occur, there would have to be a localised concentration of radiogenic elements in space and time, between 15 and 18 orders of magnitude greater than that observed within the upper mantle.

Furthermore, rocks are very poor heat conductors and their heating or cooling rate is about 50°C per Ga (Ernst *et al.,* 2001). So, even if enough radiogenic heat were available it would have taken about 20 billion years to melt its surrounding rocks. Yet partial melting of the mantle and crust does occur, even though it clearly cannot be caused by such absurd radiogenic concentrations, nor via a combination of ''wet'' mineral hydration and rapidly falling ambient confining pressure.

The estimated global production of magma and lava is just 4 km^3 annually (Crisp, 1984), or about 127 m^3/s ($\sim 4.2 \times 10^5$ kg/s), and the required energy for this is $\sim 8.4 \times 10^{11}$ W/kg. On the other hand, the Laki and Grimsvotn eruptions (1783–1785) in Iceland had an average rate of basalt production of 2300 m^3/s (Thordarson & Self, 1993), or about 18 times the annual average cumulative rate. Therefore, unless there is a geodynamic mechanism, which concentrates such tremendous amounts of energy in space and time, no partial melting can begin in the first instance. Then, the more energetic the event, the greater the dynamic energy concentration, storage containment, and sudden cataclysmic release required for it.

Similarly, for the generation of an earthquake, an energy concentration within the active volume in the range of 10^6 W/kg is required, i.e., the actual demand of power accumulation, concentration and storage is at least eighteen orders of magnitude greater than the total power radiogenic heat sources could possibly provide (Table 3). Therefore, in both cases, the implication is very clear. Volcanic and seismic events demand intense localised spatial and temporal concentrations of power, and the greater their magnitude, i.e., the size of the active volume, the greater the required concentration and storage of that power. These extreme and unseen local prerequisites are real—non-theoretical—physical process requirements and it is this intense localisation of energy which we must account for, and which the present geoscience formalisms describe as accelerated deformation.

Compatible with a reasoned consideration of available geophysical indications, Earth's interior, and particularly its core region, is assessed to be consistent with a high-energy, high-frequency, but low-temperature state of matter. The frequencies in such a high tension-pressure state will necessarily be in the range of 10^{20} to 10^{23} Hz, several orders of magnitude higher in frequency than near-surface infrared-thermal radiation frequencies. That happens because

TABLE 3
Earth's Annual Radiogenic Power Supply Compared to Earth's Geodynamic Power Dissipation Each Year

Possible supply by radiogenic heat sources	$<3 \times 10^{-12}$ W/kg
Actual usage in seismic or volcanic events	$10^{5}-10^{6}$ W/kg

the allowed spectrum of emitted wavelengths at such high ambient confining pressures will be closer to the sub-atomic particle wavelengths, 10^{-12} to 10^{-15} m, and equivalent frequency scale. Similarly, the very short-range binding energies of nucleons are in the range of millions of electron volts, compared to tens of eV for atomic orbital electrons. Thus, an atomic transition might emit a photon in the range of a few electron volts, in the visible and/or infrared light region, whereas high-energy (small scale) nuclear transitions require, and also emit, gamma rays, with characteristic quantified energies in the MeV range.

The combined logical implications of the observations presented in Tables 1, 2, and 3 lead us naturally and simply to the only physically congruous proposition left to us: that high temperatures and associated igneous melting must surely only be possible in small isolated areas within the upper-most outer "shell" of Earth, i.e., very close to its surface. Such igneous and accompanying metamorphic and hydrothermal processes, as well as asymmetric heat flow patterns, are attributed to highly concentrated electromagnetic phenomena. The localised heating of near-surface rocks is associated with electron accumulation at high local densities, temporary electron storage, and eventual accumulated voltage discharge, once the electromotive-force pressure induced by the mutual repulsion between confined electrons overcomes the localised electrical impedance to free electron flow. Associated with this process is intense radiation emission in the infrared bands ($\sim 10^{12}$ to $\sim 10^{14}$ Hz). A much simplified conceptual metaphor can be seen within the electrical impedance of a copper element in a water heater, which resists electron flow through it, thus vigorously heating the copper directly and its container indirectly, which then emits thermal infrared radiation into its surroundings.

Freund's (2003) experimental work confirms the infrared radiation emission nature of such geodynamic anomalies and processes. It is therefore logical that Earth's geodynamics are driven by electro-motive force (EMF), or rather, electromagnetic anisotropic concentration processes, and surely not by the conventional physically inadequate heat-engine bulk convection formalism. In other words, volts and amperes control tectonism and all geodynamic phenomena, on local scales, but these local scales sum globally to produce what we observe at the macro-scale.

The Conventional Problem of the Horizontal Movement of Plates

Plate tectonics hypothesis attributes geodynamic phenomena to the thermally driven density-difference–inducing convective movements of rigid "lithospher-

ic'' rock ''plates'' and associated mantle rocks below them, around a spherical planetary surface. Previously, the rock plates were considered to be about 100 km thick and decoupled or detached from the denser mantle rocks they ''floated'' on. More recently, though, plates are being treated by convection advocates as being directly and continuously coupled to the mantle rocks below them as one rock unit; a single solid contiguous overturning convection cell, which includes continents as well. Whether decoupled at ~100 km, or at some other depth, continental or oceanic plates are ideally thought to ''drift'' raft-like, diverging and converging, as otherwise insignificant skins of deep convection cells, which finally sink through the ''asthenosphere'' layer; itself a contiguous part of a viscous rock mantle. This alleged process is all ... supposedly ... due to a mere thermal-induced localised density difference gradient between rocks at different temperatures, leading to the gravitational overturn of many billions of cubic kilometers of a crystalline, high-rigidity, covalently bonded solid matrix.

It is an established fact, however, that there is not any physically observed discontinuity between deep crust and upper mantle at around 100 km depth, and the continents are observed to have contiguous mantle rock roots extending as deep as 600 km (Grand, 1987; Grand *et al.,* 1997). So the question is naturally raised: How is it possible for the upper 100 km of a continent, e.g., North America, to move horizontally by several thousand kilometers at all, under any circumstances, when global seismic tomography data indicate deep continuous roots from the surface down to 600 km depth? In other words, all of the geophysical data available to us (and ordinary classical mechanical common sense) indicate there is no such decoupling or detachment, nor independent movement of the upper ~100 km of rock, with respect to its underlying mantle rock. We would then logically have to take the position and ''accept'' that the whole 600 km depth of rock has to move en bloc, or rather, does not move horizontally to any significant extent.

But then, the whole conventional mental conceptual picture of drifting and decoupled rigid lithospheric plates, making up Earth's mobile skin, geodynamically ''sliding'' over—or with—a convecting, thermally-driven bulk overturn of entire mantle cells, falls apart completely. However, this whole ''decoupled'' plate tectonic geodynamic model formed the entire underpinning interpretive conceptual ''logic'' for the previous 40 years. It was, also, the very cause and reason for plate tectonics existing, or ever becoming such a popular, consensually acclaimed, and as yet unrectified ideological blunder. A full break with this stagnant idea of a heat-driven convection is what's required.

The Problem of the Subduction of Plates

If we, for argument's sake, accept that decoupling and horizontal movement is, however, possible, the following question is raised: How is it possible for a lithospheric plate even to begin to gravitationally ''sink'' into the mantle at all, due to a marginal density difference gradient? This would require that the plate be metaphorically as hard as a nutshell and dense as lead, and for the mantle to

be softer than butter. The actual physical data from seismic wave propagation distinctly indicate that both materials have approximately the same mechanical properties, namely, both are solid, of similar density, stiffly rigid and basically, mechanically unyielding materials, at the scales involved in geotectonics. The viscosity and rigidity of the crust and the mantle is higher than 10^{20} Pa.s and 10^{10} Pa, respectively.

These values materially approximate well only with plastic solids; furthermore, these properties of mechanical stiffness and decreasing deformability are observed to increase with depth, i.e., the material becomes even more rigid and harder to mechanically deform as depth in the mantle increases. The deformational introduction of one solid into and through another solid, as per alleged subduction settings, cannot occur unless the energy required to overcome the tremendously strong net inter-atomic crystalline bonding forces which hold the rock's atomic solid-state matrix together is somehow directly provided, when and where it is needed, in time and space. For example, the electrostatic attractive force between an electron and a proton is 10^{39} times stronger than their gravitational attraction. That is because gravity only effectively dominates energy processes on the larger cosmic scale, i.e., 10^{25} m, while the much more concentrated short-range electromagnetic force overwhelmingly dominates and is effective only at a particle's quantum electro-dynamic interaction scale of about 10^{-14} m distance between quantum particles. It is not physically possible for a nail or a bullet projectile to gravitationally sink into the interwoven bonded cellulose matrix of a piece of wood, simply because it is denser than the wood and also has a small sectional area. The scale of the nail is far too small for gravity to make a difference, even after a very long time of applied gravitational force. Only if the nail receives a sudden concentrated overwhelming energy impulse, a ''hammer blow'', can penetration occur.

More realistically, the appropriate and credible physical metaphor of subduction would be of a wooden nail being projected very slowly into a cannon ball. This is, of course impossible, even over infinite time; but even if the wooden nail were to suddenly receive such a hammer blow, required to project it into the steel sphere, the energy impulse gradient itself would simply incandescently disintegrate the wooden nail at the surface. The steel sphere may oscillate minutely, but otherwise would not be penetrated or deformed by the shattered nail.

The Physical Meaning of Elasticity, Plasticity, Rigidity, and Viscosity

Elasticity is the mechanical response of a continuous medium with inertia, while slip along a fault plane is the mechanical response of a discontinuous medium without inertia along the fault plane. Inertia, that is, mass and its continuity, are the two sine qua non of elasticity—they are always present together. Internal friction, an aspect of which is rigidity, is a combined measure of both elasticity and continuous mass. Without a medium with inertial mass and continuity, the

necessary compression and extension that produce a sine wave pulse propagating with characteristic speed within that particular medium cannot occur.

Infinite mass-inertia is equivalent to infinite rigidity, and therefore flatness, i.e., an inability to oscillate or ''wave'', a zero motion condition. But a motionless state is not a permanent absolute state in space; it only momentarily occurs during polarity changes. This reasoning gives a physical meaning to the notion of relativity and to the lack of any absolute reference frame in a finiteless cosmos.

Conventionally, the rigidity modulus, μ, is the amount of resistance, in the unit of time, with which a body opposes change of shape from a tangential-shear stress. In other words, it is the physical property of being stiff, and of resisting bending over time. It is the opposite of flexibility, ductility, malleability, or softness. However, this could be a misleading definition since the estimated rigidity of all materials when they exhibit elastic behavior is about the same, e.g., for water 10^9 Pa, for rock 10^{10} Pa. Nonetheless, liquids appear to have no effective rigidity for impulses with periods as low as 10^{-12} s, and their P wave velocity, instead of being equal to $V_P = [k + (4/3)\mu/\rho]^{1/2}$, is equal to $V_P = (k/\rho)^{1/2}$, where k is the incompressibility modulus, that is, resistance to volume change caused by a normal stress. The implication is that for oscillations with frequencies less than 10^{12} Hz, water lacks effective rigidity, because the substance's relaxation time is shorter than the applied shear stress rate.

The relaxation time is an emergent property of the viscosity/rigidity ratio; thus viscosity, or internal friction, is rigidity multiplied by time. Actually, the relationship between rigidity and viscosity is the same as between power and energy, or between motion at constant speed—which also includes the no motion state—and accelerated motion. It is important to note that material viscosity is practically indifferent to normal stress below the incompressibility threshold, but is highly dependent on temperature. It falls exponentially, and on average, by about 2% per degree C for solids and liquids, and, due to more frequent collisions between neighboring molecules, it inversely increases for gases. Air has a very low viscosity of 10^{-5}, water 10^{-3}, oil 1, mafic lava 10^3, andesitic lava 10^6, felsic lava 10^{12}, while the viscosity of intact continuous rock is of the order of 10^{20} Pa.s or higher. Correspondingly, the relaxation time of water is 10^{-12} s, of lava 10^{-7} to 10^2 s, while for rocks it's in the range of 10^{10} s. Rigidity and viscosity, as power and energy, can only occur in the presence of mass-inertia, and are actually physical measures of it. A concentration of power that exceeds the resistance threshold of concentrated mass-inertia is required in order to ''activate'' the innate elasticity within every plastic solid medium.

Consequently, the higher the effective rigidity, the higher the elasticity when transient activation energy is added, i.e., the higher the tension, and therefore the frequency of the transmitted wave in the medium, but also the higher the plasticity, which is a measure of its mass concentration, or rather, its density. This logic is confirmed by theory in the quality factor, Q, formula, $Q = \pi f/b$, whereby Q is proportional to frequency f, which is a measure of elasticity, and inversely proportional to the damping coefficient b, which is a measure of

plasticity. Also, and most importantly, this is confirmed by observation of deep earthquake seismograms, where the first motion of a P wave is evidently lossless (effectively without resistance), sharp, and of high amplitude, which then quickly attenuates as elastic wave resistance emerges.

Effective rigidity, therefore, is a measure of tensioned state in a continuous medium and of the so-called restoring force (resistance), which in turn is proportional to the mass concentration involved. The fact that rigidity is a measure of tension, and that elasticity and plasticity change in tandem, is manifested in the seismic wave speed equation, e.g., $V_S = (\mu/\rho)^{1/2}$, where μ is rigidity and ρ is density. Similarly, the characteristic speed with which a wave pulse travels along a tensioned string depends on the elastic tension-restoring force and the inertia-mass per unit length, according to speed = (tension/inertia)$^{1/2}$.

Each tensioned continuous massive medium naturally has a characteristic maximum speed with which a wave pulse can be transmitted within it, the unsurpassed maximum being the 2.99792458×10^8 m/s of light in the continuous finiteless ''free space'' medium it travels in. For example, within Earth's rocks, the transmission speed of an S wave ranges from 3 to 7 km/s. If we take the average V_S value of 5 km/s and a density of 4×10^3 kg/m^3, the rigidity should be 10^{11} Pa, i.e., the rigidity/density ratio is a constant, 2.5×10^7 m^2/s^2. The acceleration imparted by a ''net force'' will increase proportionally both the density-inertia and the rigidity-tension–restoring force, so that the rigidity/density ratio for that particular medium is always a constant. The quantitative effect of the ''unbalanced excess force'' will be manifested by the frequency increase of the emitted and transmitted wave and the increased quantity of radiated elastic wave energy.

Thus, low effective rigidity substances can exhibit elastic and brittle behaviors, that is, radiate seismic waves, but also break when two conditions are first satisfied: (a) the duration of the applied stress is shorter than the medium's relaxation time; and (b) the applied stress exceeds the shear strength of the medium, strength being another aspect of friction-inertia that refers to the inability of the medium to ever deform faster than its maximum characteristic deformation rate can accommodate.

The Least Elastic Crust, the More Elastic Mantle, and the Most Elastic Core

In the context of plate tectonics and the present elastic rebound view of rock deformation, of stress accumulation, elastic storage, and sudden release, the crust was considered as the most elastic of Earth's rock material. But inescapably, for crustal rocks to actually be the most elastic in practice, it must also logically be the most rigid, and of course, a continuous solid rock material. But this cannot possibly be the case, for it is common knowledge that the continental crust has the very lowest rigidity and density of Earth's solid rock mass and is riddled with small and long faults on all scales, i.e., it is full of discontinuities to a degree far greater than any other part of Earth's solid rock

mass. The very low Q value of crustal rocks is a measure of their lack of relative rigidity, continuity, and elasticity when compared to deep mantle rock Q values.

In accordance with this physical state, the velocity of seismic waves has its lowest values within Earth's crust, and it increases progressively as depth increases and as rock continuity, rigidity, and elasticity increase. For example, according to the Preliminary Reference Earth Model (PREM) that was created by Dziewonski and Anderson (1981) and still is the basis of all reference Earth models, the velocity of P and S waves in the upper-most crust is about 5.8 and 3.2 km/s, respectively, while at the mantle-core boundary they reach 13.7 and 7.3 km/s, respectively. The linear dependence between velocity (V_p) and density (Birch's law) actually produces a closer molecular-level material compaction with growing depth, and therefore an inter-atomic electronic pressure increase effect, and of course, higher inertia-density. Given the fact that V_p is inversely proportional to density, the increase in both rigidity and incompressibility clearly controls wave transmission velocity increases with greater depths in Earth.

But in contradiction, temperature would logically have a reverse effect, i.e., decreasing rigidity, higher solid-state fluidity, and lower density, but the observed increase in seismic wave velocity with depth clearly indicates that temperature does not continue to increase with depth in the deep mantle. Temperature's effect would be to increase the net kinetic vibrational mobility of all atoms, and therefore it would decrease the medium's viscosity, which is insensitive to pressure, and consequently lower the effective rigidity of the material—but increasing seismic velocity with depth completely disallows the popular ideal of increasing heat with depth. Furthermore, Constable and Duba (1990) demonstrated that the orders of magnitude higher conductivity of upper mantle olivine disappears at temperatures above 700°C, giving merit to the notion of a relatively cool to cold and also electrically conductive silicate rock mantle. Thus, evidence indicates that the mantle is certainly not hot at depth and becomes increasingly denser and implicitly more rigid and electrically conductive with depth. As a result, the ambient emitted and transmitted frequencies also rise as depth increases, due to higher medium tension and higher molecular compression.

Moreover, the quality factor, Q, for P and S waves, i.e., the ratio of energy stored over energy dissipated during one cycle, is proportional to frequency and inversely proportional to damping coefficient, as per $Q = \pi f/b$. The quality factor for P waves, Q_P, has its lowest value of just about 100 in the low-density crust, a high value of ~5000 in the solid and dense mantle, and its highest value on the order of 10,000 in the denser outer core (Bolt, 1982).

A measure of potential energy stored is elastic tension, and the measure of tension is the frequency of emitted waves. Frequency of emission, in turn, is a measure of the degree of elasticity-rigidity-incompressibility. On the other hand, the damping coefficient is a measure of plasticity-viscosity–mass density–inertia. It follows, therefore, that in continuous solid media, tension and mass density increase together, and this can be a physically congruent explanation as to how elasticity and plasticity increase in tandem. The increase in elasticity-

tension has a more profound effect on wave transmission velocity and energy stored. The fact that the higher the Q value the higher the energy stored is attributed to the concentration of the same energy quantum into a smaller, more intense, shorter wavelength (higher frequency) with increasing depth. In other words, the same energy quantity is pressurised into smaller volume, the size of which is a particle's wavelength. Thus, the deeper you go, the higher the energy density and the higher its characteristic black-body emission frequency spectrum, with lowered propensity for thermal photon emission, transmission, or vibratory kinetic conduction between atoms. Atomic freedom to move in thermal vibratory oscillation gets shorter and shorter in wavelength, due to the rising incompressibility of solid matter as mantle depth increases.

As vibratory oscillation reduces, the solid mantle will inevitably grow cooler with depth, a result which is consistent with seismic data showing increasing elastic moduli and wave velocities with increasing depth. Should one baulk at a counter-intuitive suggestion because of the near-surface geothermal profile and mere conditioned intuition and thermal idealism? If we consider rational observationally constrained empiricism to be a valid approach in physical inquiry, then we won't allow historical intuitive ideals to govern thinking. We emphasise, Earth's mantle is first and foremost a quantised solid-state system, where classical thermal dynamic concepts are unjustified and unconvincing. Earth must logically have a cool deep interior and electronically heated outermost solid low-pressure layer, which can accommodate and sustain elastic thermal vibratory oscillation movement of atoms in silicate crystals.

In that context, rigidity, μ, and incompressibility, k, should and do increase with depth. For example, according to the PREM rigidity from about 3×10^{10} Pa in the crust increases to 3×10^{11} Pa at the mantle core boundary, at a depth of about 2900 km, and has the remarkable value of zero in the liquid outer core. Similarly, incompressibility increases from about 10^{11} in the crustal rocks to more than 10^{12} at the Earth's center.

The rigidity of the crust is further reduced because, as it has been experimentally shown at lithostatic pressures lower than about 10^9 Pa, or rather, at crustal depths shallower than ~33-km, microcracks in rocks can remain permanently open and also may act as resonant cavities for waves, the wavelength of which is smaller than the size of the microcrack. Such permanent crustal cavities mean the Earth's crust is somewhat porous, and this is confirmed by water found by deep continental drilling projects down to >10 km. Below ~33 km depth, their temporary existence requires internal pore pressures, or harmonic resonance energy levels, which exceed the rock overburden weight.

So, the characteristic regional seismic high-velocity or low-velocity zones in the mantle are indicative of greater or lower rigidity/incompressibility and also density, and/or of the absence or presence of fractures, respectively, and not of lower or higher mantle temperature, as the standard model incorrectly attributes. But even if the Q factor were considered a temperature indicator, because Q has

its lowest value in the crust, so high temperatures in the crust and low temperatures in the mantle should be accepted, contrary to the preconceived, though actually irrational hot interior ideal.

The logical implication of all this is that the elasticity of the mantle is far greater than the elasticity of the crust, where, in actual fact, most earthquakes occur. Thus, the relatively pliable and porous crust of Earth is inevitably the least elastic medium of Earth's rocks, in conflict with elastic rebound theory, which renders the elastic lithospheric mechanics of the conventional plate tectonic geodynamic model logically and physically inoperable and profoundly in error.

An earthquake mechanism other than the crust's non-existent greater rigidity and effectively weak small-scale elasticity has to be responsible for the concentration of the bulk of recorded earthquakes within the thin, locally heated, porous and discontinuous outer skin of our planet. Implicit in this preceding statement is the recognition that observable aseismic creep within a known active fracture zone does not and cannot equate to accumulation and storage of elastic stress over time and then a sudden release of it seismically.

Static Stress Changes Along Faults Do Not Produce or Trigger Earthquakes

Static stress is a stress which is constant, or slowly increasing, with time and that can actually produce rupture, but that cannot mechanically induce a true adiabatic deformation. According to mainstream theorization, though, static stress changes along faults produce frictional sliding on a fault plane, eventual regional failure, and then formation of a true earthquake shock.

In the expected conventional context, if the earthquake is large enough it can influence the spatial and temporal distribution of regional seismicity. Its redistribution effect depends on the fault geometry and accelerates proximal seismic activity in areas of resulting static stress increase, although it decelerates it where static elastic stress has been relieved (Figure 1a).

The Coulomb failure criterion requires that both the static shear and normal stress on an incipient fault plane satisfy conditions analogous to those of friction on a pre-existing surface (King, *et al.,* 1994), i.e., a weakening close to failure state, which nonetheless is the opposite of the high-strength ''locked'' fault prerequisite required for high elastic strain energy accumulation in the first instance. Bypassing this obvious contradiction, and in an attempt to explain this necessary critical precursor state, the idea of ''self-organized criticality'' has been introduced (Bak & Sneppen, 1993; to 1995). According to this general idea, somehow (but how?) all parts of the ''brittle'' crust are at the point of failure, and some distant events may be triggered by stress changes as low as 0.1, or even 0.01 bar.

But ''Seismologists have never directly observed ruptures occurring in Earth's interior. Instead, they glean information from seismic waves, geodetic measurements, and numerical experiments'' (Kanamori & Brodsky, 2001), or

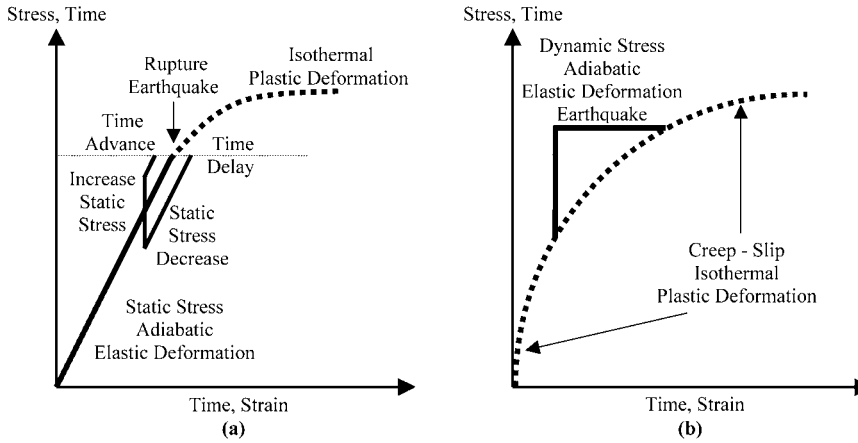

Fig. 1. (a) Conventional elastic-plastic deformation with static stress accumulation and transfer along a fault plane within an elastic medium; (b) Proposed plastic-elastic-plastic deformation and dynamic stress within low-elasticity microcavity networked plastic medium.

statements like ''An isolated fault has never been observed!'' (Sornette, 1999). Also, Knopoff (1999) notes, ''Seismicity at almost all scales is absent from most faults, before any large earthquake along that fault. The San Andreas Fault in Southern California is remarkably somnolent at all magnitudes on the section that tore in the 1857 earthquake'', and ''there is no evidence for long-range correlations of the stress field before large earthquakes''. Likewise, Chinese scientists have noticed the remarkable lack of correlation between fracture phenomena and surface tectonic features, with seismogenesis, which is attributed to deep sited on-going activity within rift zones (Shih *et al.,* 1978).

Therefore, the doubtful assumption of an elastic crust, in which elastic strain accumulates over time in the focal region of a future earthquake, is actually not verified by observations and cannot provide any realistic assessment of relative earthquake potential. In other words, contrary to all expectations, we do not have any known cause-effect relationship between fault existence or recent activity and its future earthquake potential. Faults, whenever present, are a secondary post-seismic effect, and not a pre-seismic factor in their occurrence or recurrence.

The January 19, 1968 ~1 MT, 1 km depth, thermonuclear test at the Central Nevada test site, given the code name ''Faultless'' before it took place, produced a fresh fault rupture at the surface about 1.2 km long (Bolt, 1976). In this same ''Faultless'' nuclear test, another observation of great importance was made. The seismographic records showed that the seismic waves produced by the fault movement were much less energetic than those produced directly by the explosion itself. The implication is clear. Static stress changes along faults can only produce relatively minor to almost undetectable tremors, but no full elastic shockwave response. Instead, an almost instantaneous high stress rate is required

for the generation of a shock front, and the more so for a moderate to major earthquake.

After this ''Faultless'' nuclear blast, the Central Nevada site was considered unsuitable for high-yield testing, which lead directly to a five times larger 5 MT underground test called ''Cannikin'', in the isolated Aleutian Islands. This test conclusively showed that artificial earthquake shocks, caused by particularly energetic thermonuclear explosions, have not been observed to trigger sympathetic earthquakes. The ''Cannikin'' test occurred on Amchitka Island, midway along the arc of Alaska's Aleutian Islands, on November 6, 1971, and was the U.S.'s largest historical underground test, with a body wave magnitude of about 7. If such powerful shocks could trigger sympathetic elastic strain release, then it could be reasonably expected that a shock with a prompt measured ground uplift about 7 m would produce correlated shocks in the following time. But, it did not increase local seismicity at all, in an area where crustal seismic swarms were very common. Hence, large seismic shocks are not the cause of smaller temporally and spatially correlated shocks. A different primary mechanism must be responsible for each, of which both shocks and fault ruptures are geodynamic symptoms—and are not considered causes of each other's occurrence.

Solids could be treated as ideally Newtonian, i.e., stress and the infinitesimal strain are proportional; but in experiments, loaded rocks, due to accumulated fatigue and/or progressive creep failures, actually behave as non-Newtonian plastic solids. Thus, shear compliance increases with time as the rock's character evolves in response, and rocks can fail without any shock impulse at all, when the strength of the rock has been significantly reduced by the enhancement of microcracking, produced by the constant application of a static stress, even if the applied stress is significantly below the normal shear strength for the rock (Figure 1b).

Freund's experimental work (2002, 2003) with projectile impacts to a granite block ($25 \times 25 \times 20$ cm^3), showed that an 1.45 km/s impact velocity generated P and S waves propagating at about 6 and 3.4 km/s, respectively, that soon died down within 200 μs after impact. At 4.45 km/s, impact fissures began to form 2 ms after impact, which is an order of magnitude later in time after the fade out of the impact's oscillatory wave movements, while at 5.64 km/s, the block ruptured into three segments along the formerly formed fissures. In a medium with limited rigidity, the impact caused the instantaneous exceeding of the total inertial resistance in the entire volume of granite block, which losslessly accelerated it in the first cycle to the maximum allowable seismic wave speed in that medium. After that, due to the instantaneity of the acceleration and the continuously decelerating effect of the rock's inertial mass, the oscillation is damped out as it exponentially attenuates to ambient levels of noise.

Conversely, static stress experiments have shown that if the yielding strength is surpassed, at first wrinkles, and finally a conjugated X-shape fracture system, develop (Chang & Zhong, 1977).

Shockwaves, Elastic and Non-Elastic Strain Rates

Like evaporation, aseismic, inelastic creep is slow—slower than relaxation time, or isothermal deformation with characteristic inter-atomic re-crystallisation deformation of the petrofabric. The kinetic energy, coming from the outside, is transformed into kinetic friction heat at the leading surface of contacts between two slightly separated petrological boundaries. The extremely low stress drop values indicate that there is very minimal elastic strain accumulation possible as well, because mineral re-crystallization quickly results, thereby both consuming and relieving internal elastic strain energy growth, plus changing the nature and preferred mineral orientation and resulting cleavage planes within the rock.

The shear compliance will of course increase as the frictional resistance between crystals is drastically reduced over time, or if an external directed stress is suddenly added. For a rock rigidity of 3×10^{10} Pa, a weak "secular" stress, of the order of $\sim 3 \times 10^{-4}$ Pa/s (10^4 Pa/yr), will produce creep rates in the order of 10^{-14}/s that correspond to a constant velocity of about 3 cm/yr (10^{-9} m/s), of the conventionally supposed 100 km thick slabs of plate tectonics. This creep rate and the estimated stress drop in minor and major earthquakes, from 10^4 to 10^7 Pa, and the coseismal slip rate in big earthquakes, of the order of 10^{-4}/s or even higher, if the rigidity is 10^{10} Pa can be logically attributed to a dramatic stress rate increase to 10^6 Pa/s, or to an equally dramatic reduction of rigidity to 1 Pa, for a 10^{-4} Pa/s stress rate. It is important to note that the 10^6 Pa is still at least two orders of magnitude lower than the average strength of rocks. But the reduction of rigidity likewise brings on a decrease in achievable elasticity, and typical P and S wave seismic propagation velocities require medium rigidities well above 10^{10} Pa. If, however, rock rigidity is not less, then an actually realistic process for the generation of the high stress rate shock induction within otherwise plastic rocks must be proposed.

The implication is again clear: Rocks under constant stress do not, and actually cannot, respond as Newtonian elastic media, but thereafter as static stress application, only as non-Newtonian plastic solids (Figure 1b). Both creep and slip are isothermal, non-elastic deformations, and cannot and certainly do not produce major earthquake shocks, as the nuclear test explosions showed. All rocks, like all other covalently bonded solids, can be made to momentarily deviate from their routine plasticity and suddenly respond elastically—namely as true Newtonian elastics which losslessly accelerate, if they are subjected to a sudden stress rate, such as a nuclear detonation stress rate. A plastic solid material will not deform elastically if the stress is below its inertia threshold for shockwave response. When this threshold is exceeded, however, velocity will increase linearly with time, and strain with the square of time, thus implying constant acceleration of a true, though temporary, elastically responding rock medium.

In our reasoning, as shown in Figure 2, a traveling wave within any medium always carries with it an integral standing wave structure which is holding its propagation and oscillation velocity back to a constant. A standing wave

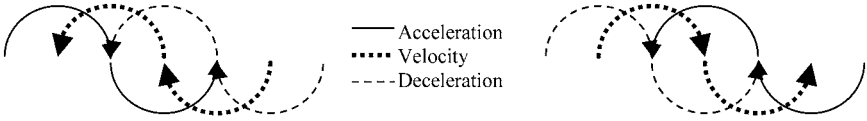

Fig. 2. Any traveling wave, be that a photon or a seismic wave, moving at a medium's characteristic speed, i.e., the maximum elastic deformation rate for that elastic medium, after the initial first oscillation cycle; it carries within it an integral standing wave form-"matter", caused by the mediums inertial elastic deformation response.

imbedded in a continuous elastic medium with infinite elasticity, such as "free" space logically exhibits, given its observed wave-particle contents and behaviour, is what we call "matter". Moreover, this tensioned infinitely elastic continuous space gives to inertia its actual physical meaning and expression, i.e., a traveling wave in any medium cannot travel faster than a characteristic finite maximum deformation speed for that particular medium. That because at the instant of the attempted wave speed transcendence we have conditions analogous to a wave pulse on lossless, constant length tensioned elastic string, approaching a fixed end. The internal restoring force, which is actually inertial mass in every type of natural waveform, exerts an upward "force" on the end of the string. But, since the end is rigidly clamped, it cannot move, and reflects the energy imparted to the end. According to Newton's third law, the wall must be exerting an equal downward force on the end of the string. This force creates a wave pulse that propagates in the opposite direction with opposite wave polarity, but with the same speed and amplitude as the incident wave—it is essentially and actually the perfect reflection of the original wave. So, the original incident and returning reflected wave form a standing wave structure along the losslessly oscillating tensioned elastic string.

A traveling wave, e.g., a photon, carries with it an integral standing wave structure, a particle, and travels with an inevitably finite and constant speed, characteristic of that perfect elastic medium. In the absence of physical inertial mass of the medium, which is "space", both acceleration and velocity could actually acquire quantitatively meaningless infinite values. But in the continuously oscillating, at light speed ($v = c$), space-medium with actual physical mass per unit volume, the inertia threshold, external acceleration, and inertial acceleration and, of course, deceleration, can be regarded as absolutely 2.99792458×10^8 m/s^2. Such a perfect elastic space itself will not allow any wave within it to oscillate or propagate faster than 2.99792458×10^8 m/s within its own inertial frame. So, matter's inertia, i.e., the number of standing waves the matter consists of, quantitatively determines the elasticity threshold, the wavelength, and the maximum deformation rate of an emitted traveling wave.

For a perfect-elastic finiteless continuous medium, such as "free" space is, due to its infinite rigidity and lossless reflection of waves which are attempting to exceed the maximum deformation rate, c, external and inertial acceleration

and inertial deceleration are of course going to be exactly equal and also lossless, within each and every elastic wave cycle. In other words, the wave structures themselves would never attenuate, even over infinite time.

On the other hand, in the event of an effectively elastic rock, with a finite rigidity of 10^{11} P and density 4×10^3 kg/m^3, only the first wave oscillation cycle will be lossless. In that medium S waves cannot travel faster than 5 km/s, which is the elastic wave medium's own integral limiting maximum deformation and propagation rate, without breaking its continuity. As a result, a high-pressure/high-density/high-rigidity front is produced that explains the shockwave characteristics of any seismic source's mechanism, and explains why the V_S : V_P ratio is 1 : $\pi/2$, or ~0.6366, while any lower values are attributed to smaller or larger discontinuities in the medium (Figure 3a).

Thus, a ''free'' lossless elastic space and rocks differ as well in that space would exhibit infinite rigidity (energy reflecting non-deformability) for speeds faster than light speed, and as a result, space's physical continuity could never be disrupted, nor made discontinuous via fracture (Figure 3b). But rocks have only a finite rigidity, and if the wave source's speed exceeds the characteristic traveling wave speed the rock can put up, the rock medium will rupture at that point, producing a fault (Figure 3c).

An earthquake, as with melting and boiling phase transitions, requires the appropriate acceleration-''net force'', in order to instantaneously overwhelm the internal bonded crystalline energy threshold of any rock, which actually is the so-called latent energy of about 2×10^6 J/kg. That energy corresponds to a ''net force'' of 2×10^6 N/kg, or to a speed of ~1.4 km/s, and an acceleration ~1.4 km/s^2 of 1 kg of mass, or to a speed of 1 m/s and acceleration 1 m/s^2 of 2×10^6 kg, the latter being closer to reality. The energy discharged into a plastic solid will force it—or, more correctly, shock it—into responding instantaneously elastically, thus naturally leading to the generation of an earthquake's necessary shockwave front (Figure 3a). The faster the adiabatic shock stress rate, and/or the greater the volume it occurs within, the greater the magnitude of the inevitably resulting earthquake. But, the elastic response of the otherwise plastically responding rocks is only for one cycle. After the first cycle the oscillation will attenuate exponentially due to the medium's intrinsic inertial mass resistance.

The shockwave pressure, ρV_S^2, of 10^{11} Pa, caused by the sudden impact on a rock with $\rho = 4 \times 10^3$ kg/m^3 and $V_S = 5$ km/s, thus generates earthquakes, and can subsequently rupture rocks if the rock's effective mechanical wave elastic bond strength is exceeded (Figure 3c). This can occur where an adjacent volume's frictional resistance is reduced, e.g., to 10^9 Pa; then, even if its density is also significantly reduced, the allowable S wave propagation speed will be about an order of magnitude lower than the speed of the effective seismic wave source velocity, which was a rock with 10^{11} Pa rigidity. As a result, the rock will naturally rupture at the impedance boundary region between the two rigidity-differentiated volumes. It is obvious, therefore, that unless the condition of lower effective rigidity in an adjacent volume is satisfied, fault rupture will not ensue and the

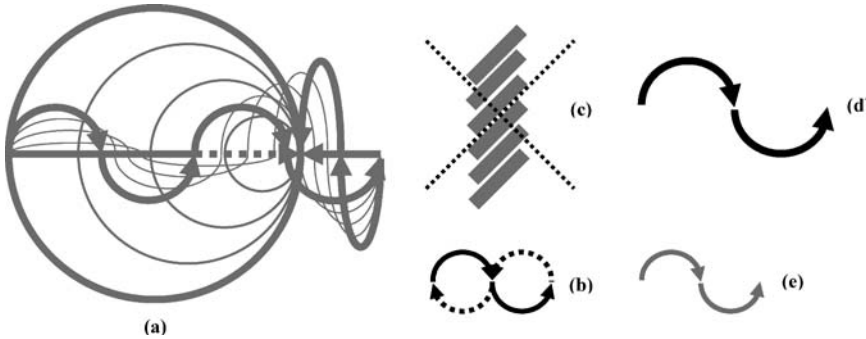

Fig. 3. A transverse S-wave if extended to flatness, that is by $\pi/2$, or $\sim$57% (dotted horizontal line), by a sufficiently high energy/momentum impact, required to overcome the inertia of the standing wave-matter it is imbedded within, a shockwave, i.e., a longitudinal P-wave, is thus produced, so that VS : VP = 1 : $\pi/2$ ($\sim$1.57), and an earthquake shock is likewise generated. Note that the ''blue shifted'' wave amplitude (compressed sine wave outside the circle) to perfect sine wave amplitude ratio is exactly 2:1 (a). In the case of Z_∞ space's infinite rigidity of a literally infinite, continuous and perfectly elastic space with its own intrinsic mass, a rupture of space can never occur from a shock impulse, and at accelerations which might attempt to exceed light speed, a resulting lossless reflection of the elastic wave (of space momentum) occurs, and a matter-standing wave thus duplicates itself, but at a lower wavelength/higher frequency than the pre-reflection sine wave (b). But, if the wave's medium instead has only a finite rigidity, as do all rocks, a rupture and sympathetic fault surface can form, if the impact rate is greater than the mediums' maximum potential elastic deformation rate possible between its mineral bonding (c). In a comparison of a plastic medium with finite rigidity (rocks), and an elastic medium with infinite rigidity (Z_∞ space), transverse S-waves will be emitted if each medium is exited, the difference between them being in the emitted frequency each propagates. In the plastic medium with finite rigidity case, frequency will remain unchanged, regardless of fault generation or not (d); in the elastic medium with infinite rigidity case, frequency will be higher (e), but frequency will not and can not alter as the emitted wave propagates through it.

earthquake will not be accompanied by a fault, just as many earthquakes are observed not to.

The shockwave and virtual normal fault characteristics, indicative of vertical compression directly beneath the station network, are evident in the 3.7 ''volcanic'' earthquake recorded on June 4 1991, shortly before Mount Pinatubo exploded on June 15, 1991 (White, 1999). The arrival timings are nearly simultaneous, with the first motion of P waves emergent and down at all six recording stations, and the ground displacements are of similar amplitude at a station located 9 km from the peak, and another one located just 1 km away. The implication is of a point-like high-energy wave source that attempted, without subsequent success, to move faster than the shockwave, i.e., longitudinal, P-wave, which it finally produced (Figure 3a). If the medium has infinite rigidity at speeds that tend to exceed the maximum elastic deformation rate of it, a lossless reflection will occur, and matter-standing wave will duplicate itself, without any rupture. But, both ''new'' particles will have shorter wavelength/ higher frequency than before the lossless reflection (Figure 3b). The only

medium with such properties is the infinite continuous and perfectly elastic space with mass that exhibits infinite rigidity at speeds that tend to exceed light speed. However if the medium has a finite rigidity, e.g., rock, and, due to the appropriate proximal conditions existing, i.e., a very high stress rate, it succeeds in travelling faster than an elastic wave in the propagation medium, an actual fault rupture must form, which may also have a surface expression if the rigidity impedance difference was at or close to the surface (Figure 3c).

In both cases, i.e., a plastic medium with finite rigidity (rocks), and an elastic medium with infinite rigidity (Z_∞ space), transverse S-waves will be emitted if each medium is exited, the difference between them being in the emitted frequency each propagates. In the plastic medium with finite rigidity case, frequency will remain unchanged, and regardless of a fault generation or not (Figure 3d); in the elastic medium with inifinite rigidity case, frequency will be higher (Figure 3e), but frequency will not and can not alter as the emitted wave propagates through it.

After the shockwave has moved through, the rock will very rapidly return to its previous, solid plastic aseismic deformation existence. Freund (2002, 2003) has shown experimentally that a bullet impact upon a rock with a velocity 1.45 km/s causes a shock, and post-shock formation of P and S waves, whose role is to radiate and dissipate the near-instantaneous elastic shock energy, within 200 μs of impact. Thus, theory and observation indicate that unless rocks are subjected to a very sharp and intense point-like dynamic high-rate stress loading, an earthquake cannot and surely will not be generated. These inescapable crucial mechanical necessities are effectively ignored within the present elastic rebound models.

Spatial and Temporal Clustering of Earthquakes

It is an observed fact that, contrary to the elastic rebound-seismic gap model, according to which the repeat time of major earthquakes in a given location is on the order of thousands of years, earthquakes cluster in space and time. Earthquake swarms and aftershocks provide a familiar example, but large main-shocks are also observed to cluster (Kagan & Jackson, 1991). The implication of clustering is that, for a location, the longer you have waited since the last major event, the longer you still have to wait (Bak & Sneppen, 1993; Ito, 1995). In contrast, in the seismic gap model, the stress energy after a strong shock is regionally depleted, thus preventing future earthquakes nearby, until the stress is restored, i.e., all else being equal, the probability of a strong event recurring increases with time following the preceding event.

According to Jackson (1999), the seismic gap model has failed every prospective test applied to it. The most characteristic case is the Parkfield earthquake, which, with the estimated repeat time of 22 years, should have happened in 1988. The earthquake of 28 September 2004 occurred 16 years later. Also, a 1989 forecast predicted that nine major events should have happened by 1994 in about 100 circum-Pacific zones, but only two eventuated.

If the seismic gap model were correct, there should be a reduction of

probability for an equally strong or stronger earthquake to occur in adjacent faulted active areas, immediately after any strong event. But, according to the EQE-ABS Consulting Summary Report in 1994: ''There is no indication that the occurrence of the January 17, 1994, Mw 6.7 Northridge, CA Earthquake, has reduced the probability for a stronger earthquake in the next 30 years on a major fault in the Los Angeles region. The probabilities remain in the range of 5% to 10% per year that a major earthquake will strike Southern California''.

Logically, therefore, the observed spatial and temporal clustering of earthquakes, combined with the lack of apparent triggering connection between earthquakes, is attributed to the spatial and temporal clustering of deep-seated, internal causative agents, close to a critical, though localised, stressed state.

Earthquake Mechanics in the Context of a Solid and Quantified Earth

Before answering the question ''what are the consequences of shock stress–induced deformations of rocks'', we have to first answer a more fundamental question: ''what is the actual physical mechanism of seismic wave production which is common for all 'types' of earthquakes, i.e., tectonic, volcanic, deep, intermediate, or shallow?'' According to the standard model, the seismogenesis occurs in a microcracked seismogenic volume, which, nevertheless is still irrationally considered to somehow be a high-strength ''locked fault'', regardless of pervasive microcracks. But these two physical conditions for the seismogenic volume are logically incompatible states, hence, mutually exclusive—both cannot be true at the same time. Microcracking is a rock weakening process, but seismic wave strain rates require a strong, continuous, and competent rock medium.

If the rigidity remains unchanged before and during the earthquake nucleation process, at $>10^{10}$ Pa, in order to support observed P and S wave speeds, the demanded stress accumulation rate has to increase by 10 to 12 orders of magnitude above ambient. Otherwise, if the stress rate were to remain unchanged at 10^{-4} Pa/s, the rigidity has to drop to 1 Pa, in order to obtain a 10^{-4}/s slip rate.

The contradiction of incompatible states is this: (A) How could a stress rate rise, by so many orders of magnitude, occur, without any changes to the elastic properties of the medium? In other words, how could a weak volumetric ''secular'' normal stress rate of 10^{-4} Pa/s, acting on a medium with rigidity $>10^{10}$ Pa, very suddenly increases by 10 orders of magnitude to a 10^{6} Pa/s shear stress, which still is at least two orders of magnitude lower than the$>10^{8}$ Pa of the rock's strength, but is capable of producing 10^{-4}/s slip rates, plus seismic waves traveling at $>10^{3}$ m/s. (B) The reduction of rigidity to 1 Pa, which is the physically congruous state associated with the weakening process supposed along a fault plane, becomes then physically incapable of sustaining the seismic wave strain rates and velocities actually observed.

The question therefore is, How and why is it considered possible that a weakening process could produce high elastic potential energy storage and release over a hundred or thousand year period, when logical reasoning and

experiment say that microcrack development will have precisely the reverse effect of vastly reducing the medium's elasticity potential? And what energy, what process, could realistically cause this implied energy magnitude transition to actually occur, to force a plastic solid rock to respond momentarily like an elastic solid?

In a series of papers, Tassos (2001, 2002a,b,c, 2003) attempts to answer these and other fundamental questions and presents arguments for a plastic solid, electro-quantum process–controlled, expanding Earth. In this paper, we will waive further comment on global expansion. A thorough recent presentation of the evolution and current state of the Earth expansion research can be found within the book *Why Expanding Earth?* (2003), edited by Giancarlo Scalera and Karl-Heinz Jacob.

In contrast to the present geodynamic ideals, Earth's core, in logical compliance with existing physical evidence, is considered by us to be a highly conductive, cold, high-frequency/high potential-energy/high-tension material, in which the net synthesis of new atoms of different elements routinely occurs. Due ultimately to cosmological stretching, which continually increases the elastic tension field of the infinite continuous and perfect elastic space-medium in which Earth is embedded and consists of, Earth is likewise under constant internal space tension, the expression of which is what we directly experience and refer to using the term ''gravitational attraction''. Since the tension of stretched elastic space, which is the repository of all mass, increases endlessly with time, due to the cosmological expansion stretching of the elastic space itself, there will of course be a resulting linear frequency of emission increase from all matter embedded in that space, like a drum-skin, with time. As a result, the higher the nuclear binding energy of an atom, the later the atom will form in a particulate-wave material body, such as Earth is observed to be.

What we are seeing geodynamically today is a global solid-state ascent of iron from Earth's core, with emplacement alteration/insertion, atom by atom of this iron into pre-existing silicate rocks, both within the mantle and within differentiated crustal rocks. In short, ''Excess Mass Stress Tectonics''—EMST (Tassos, 2001, 2002a,b,c, 2003) concerns the electrical and magnetic processes which have been altering low Fe silicates into becoming high Fe silicates, and how this on-going geodynamic and geochemical metamorphosis of Earth is being expressed, in terms of geotectonism, earthquakes, volcanic-, and magmatic-related processes, throughout Earth's quantised geological history.

The binding energies of nucleons are in the MeV range, compared to tens of eV for atomic electron binding. Thus, an atomic transition may emit a photon in the range of a few eV, perhaps in the visible light region, whereas nuclear transitions can emit high-frequency gamma rays with quantum energies in the MeV range, due, naturally, to higher pervasive space tension within and around shorter wavelength and, consequently, higher frequency standing wave-matter, i.e., particles-waves.

Iron, which has the highest nuclear binding energy of all atoms—8.8 MeV per

nucleon, is also the most stable atom of all, because the construction of its nucleus, either through fusion or through fission, requires more energy than any other element, and its formation will occur, if and when that energy becomes available. Therefore, iron will be the last element to form, and the fact that most of Earth's known iron-rich rocks, such as oceanic crust, are largely younger than about 200 m.y., indicates that Earth's internal tension and energy have been rising with time, and that prevailing core energy levels now allow constantly occurring synthesis of iron atoms.

As a matter of fact, there are a series of elements, heavier and lighter than iron, the fission and fusion of which, respectively, deducts or stores, rather than releases, net energy. The yield of energy from fusion is limited to elements below boron, e.g., H^1, H^2, He^4, Li^7, and Be^9, since the fusion from B^{11} to Fe^{56} demands net free energy expenditure. Similarly, the fission from Sn^{119} to Fe^{56} would require, rather than release, stored energy. In contrast, the fission from U^{238} to Pb^{207} to Sn^{119} releases net excess nuclear energy.

In high spectral redshift stars (earlier, lower elastic space tension state stars), the build-up of heavier elements via the nuclear fusion processes is limited to elements below iron, due to insufficient quantised energy levels being available. That being so, and despite present beliefs, this is indicative of greater age and lower energy state. Actually, lower elastic tensional potential existing within those stars at that time, when compared to Earth's present iron forming, quantified internal energy state level. In that context, astronomical redshift values greater than ~0.57, are considered non-Doppler in origins.

Iron ascends from Earth's core under electromagnetic pressure, into a geologically tensional extending mantle, in the form of reduced high pressure Fe^{2-}, in which the 4s orbital is compressed down to the 3d orbital, that can then be filled with five more electrons than without compression of electron orbits. It ascends as an Excess Mass (EM) core product, in the form of solid injection ''wedges'' into the preexisting iron poor mantle and crust resulting in their ''oceanization'' (Beloussov, 1980), and which, when oxidized at lower pressures as it rises, releases its 4–5 ''excess'' electrons and thus transfers elastic tensional energy—for EM actually means excess energy, as per $E = mc^2$—from Earth's interior, toward the surface. This process of high-pressure injection and atomic and plasma rise through the mantle causes microcrack formation of near atomic size (10^{-10} m). Upon encountering a temporarily impassable obstacle, a material and electrical anisotropy within the mantle, the ascending EM Fe^{2-}, and its released excess 4–5 electrons, begin to accumulate below the anisotropic obstacle, blocking further unimpeded ascent. This increases the localised internal pressure behind the structural obstacle blocking ascension. As a result, the size of microcracks produced by intrusive emplacement increases to crystal sizes, i.e., $\sim 10^{-6}$ m.

Impact experiments demonstrated that electron injection begins at speeds from 0.1 to 6 km/s (Freund, 2002, 2003), while White (1999) calculated an ascent rate of the basaltic material from 3 cm/s to 12 m/s. Therefore, each

ascending Fe^{2-} atom can release up to five electrons, which can travel in the bulk rock at speeds in the order of 10^2 to 10^4 m/s. By releasing its electrons, the reduced Fe^{2-} turns into the volumetrically elastically expanded and oxidized $Fe^{2,3+}$, which actually is an effective p-type semiconductor, an atom which moves at much slower speeds, ranging from 10^{-2} to 10 m/s. Since electrons can travel faster than either the Fe^{2-}/ $Fe^{2,3+}$ effective p-holes, electrons arrive first at the impeding anisotropy obstacle, then flood existing silicate minerals and rocks which contain Si^{4+} and $Fe^{2,3+}$, transforming them also into ''slow'' moving charged effective n-type semiconductors.

So, ''new'' free electrons from Fe^{2-} and also ''old'' free electrons from the metallic bond of $Fe^{2,3+}$ will interact with minerals in upper mantle and crustal rocks, forming temporary n- and p-type semiconductors, but they also tend to accumulate inside low-impedance cavities opened up by the excess electron's mutual repulsive pressure behind the ascent barrier, i.e., seismogenic volume microcracks develop as a result of ascent impedance anisotropy.

Microcracks have a dual function, as resonant cavities for heat-generating resonant free electrons and as effective electrical capacitors with semiconductor behavior. It is these ''new'' released effective free electrons from Fe^{2-}, acting as a shaking force inside the 10^{-6} m microcavities, that harmonically resonate with ''old'' free electrons from $Fe^{2,3+}$ and thus radiate excess harmonic excitation energy at the fundamental frequency of $f_1 = 5 \times 10^{13}$ Hz. This frequency corresponds to a fundamental wavelength $\lambda_1 = 2L$ of the cavity, i.e., they radiate in the infrared-thermal part of the electromagnetic spectrum. This mechanism neatly provides heat energy in a highly localised, extremely energetic, but also transient form, for magmatic and volcanic activities, and explains the anomalous observed local temperature increase before an earthquake. So we propose an electromagnetically dominated, and thereby locally heated upper mantle and crust, via electrons, their resonance, and their electromotive force (EMF) pressure-driven flows; a logical, seamless, and coherent accounting of all near-surface geothermal observations, without recourse to any of the present physically inconsistent theories, or their inevitable ad-hoc ''special case'' constructions, which they continually require. The resonance of ''old'' metallic bond electrons from $Fe^{2,3+}$ and ''new'' electrons from Fe^{2-} is named Electron Resonance Stimulated by Excess Mass Electrons (ERSEME) (Figure 4).

An earthquake of magnitude 8.9, which is about the maximum known magnitude and the annual cumulative magnitude of all earthquakes, releases about 1.5×10^{18} J of elastic wave energy. This is, however, an insignificant fraction of total seismic moment M_0 (Aki, 1966). Seismic moment is a measure of total energy involved in an earthquake and the product of rigidity, μ, and the active volume, ΔV, which for an 8.9 earthquake is on the order of 3×10^{22} N.m (J). This great difference between seismic moment energy and the released elastic wave energy is due to the work required to overcome the electromagnetic and quantum-mechanical forces between chemically bonded ions in the crystal

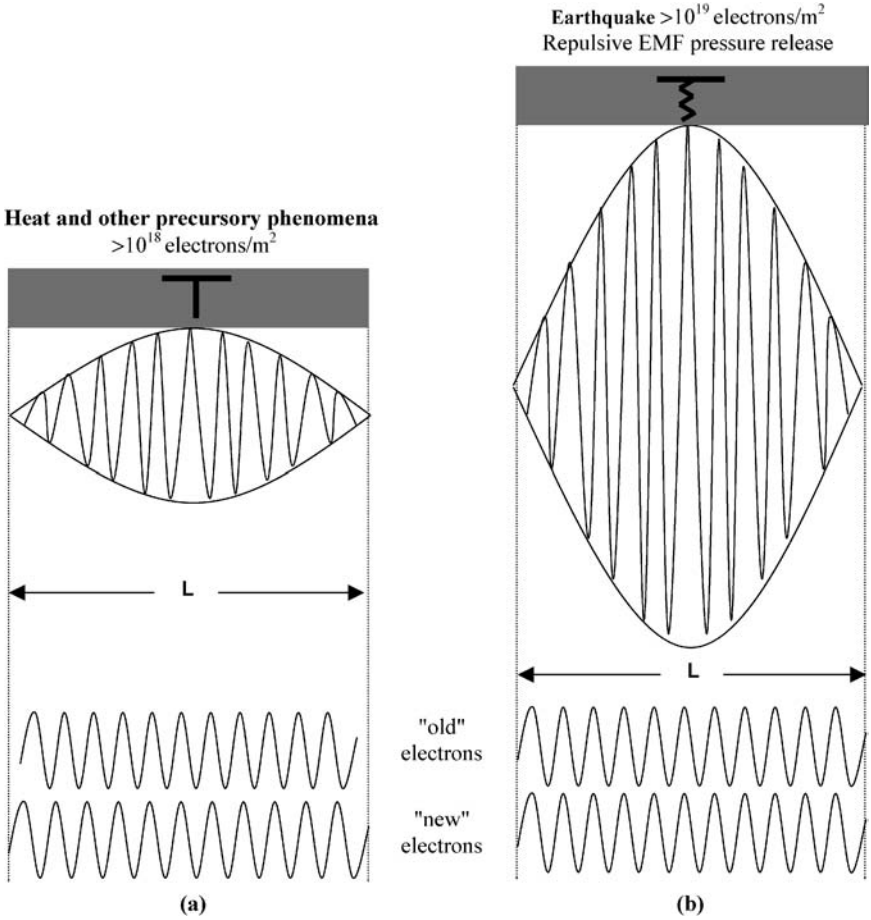

Fig. 4. The Electron Resonance Stimulated by Excess Mass Electrons—ERSEME—process and the dual role of microcracks, (a) as wave harmonically resonant cavities, where radiant heat and other precursory phenomena are produced; (b) as a network of many effective capacitors, connected in parallel electrically, the implosive gravitational collapse of which produces all earthquake shock types, whether deep-focus, shallow focus, tectonic or volcanic. $\top_{\text{Plastic solid}}$ $\top_{\text{Elastic solid}}$.

lattice within the seismogenic volume. Considering that the 3×10^{22} N.m of seismic moment and the rigidity, μ, is of the order of 3×10^{10} N.m^{-2}, then the effective-active volume change, ΔV, representing the micro-fragmented volume, of maximum 10^{30} microcracks, which are then packed full of ''excess mass'' atoms and minerals, is on the order of 10^{12} m^3, which corresponds to a cube with a side of 10 km, or to a sphere with a radius of 6.2 km.

Assuming that the average density of EM approximately equals the average density of the mantle, i.e., 4500 kg/m^3, a volume of 10^{12} m^3 corresponds to an

earthquake-related EM, Δm_e, of 4.5×10^{15} kg. The newly formed excess mass atoms and minerals that fill the microcracked volume represent the active mass.

If about one third of Δm_e is Fe atoms, i.e., 1.5×10^{15} kg, then about (1.5×10^{15} kg/$56 \times 1.67 \times 10^{-27}$ kg =) 1.6×10^{40} Fe^{2-} atoms, and about 10^{41} ''new'' electrons related to earthquake generation and radiant heat release are being added each year to Earth's rocks as EM and equivalent potential energy. This addition to the mantle and crust is where Earth's near-surface heat release springs from and why high heat flow rates are so strongly associated with the geodynamic activity, which is induced by localised intensive Fe intrusion/alteration of silicate minerals and vigorous localised electron resonance and resulting crustal heat flow.

From a simple thought experiment (see Appendix) we can see that if the number of excess electrons is better than 10^{18} parts in 1 part of ''old'' electrons, some large and mechanically significant electrostatic repulsion effects between macroscopic bodies will occur. So, the annual supply of 10^{41} effectively excess ''new'' electrons, which corresponds to an average surface concentration of more than 6×10^{18} ''new'' electrons/m^2/s, if evenly distributed, gives ''self-organized criticality'' its physical expression and energy source. If clustered in space and time, their electrostatic repulsion effects are instant and intense, creating a strong local EMF pressure gradient.

If that reasoning is correct, it should be consistent with direct observations before, during, and after a seismic event. Satellite radar interferograms, provided by the synthetic aperture radar of the European Space Agency, have shown that between two acquisitions, on August 13 and September 17, 1999, an elliptical dome ~250 km E–W, by ~60 km N–S axis, with its apex at ~75 cm, was formed as a result of the 7.4, August 17, 1999, Izmit earthquake (Hanssen *et al.,* 1999). Indeed, the excess volume, on the order of 4.4×10^9 m^3, is of the same order as the theoretically quantitatively predicted (3.3×10^9 m^3) for a 10^{20} N.m earthquake caused by excess mass stress.

Likewise, White (1999) demonstrated the direct association of the 3.7 Mount Pinatubo seismic event with the aseismic ascending of deep-seated basaltic material and estimated its effective source volume to be 2.25×10^4 m^3, both in good accord with our ''excess mass'' logic, in which the ''freshly quenched'', actually emplaced in solid state, basaltic dome itself is nothing else but a remnant manifestation product of excess-active mass and energy emplacement and ensuing release processes.

Seismic moment, M_0, is the total potential energy change and includes the frictional energy loss, E_F, some fracture energy, E_G, and a minute residual fraction of energy radiated as elastic-seismic waves as earthquake, E_R, i.e., $M_0 = E_F + E_G + E_R$, and $E_R = M_0 - (E_F + E_G)$. In the context of conventional elastic rebound, thermal frictional energy is the energy spent to overcome kinetic friction, and large earthquakes occur on well-developed and/or ''lubricated'' faults (Kanamori & Brodsky, 2001). Such faults do not use much frictional energy making new surfaces, as non-lubricated faults in small earthquakes do, thus leaving more energy to be radiated as seismic waves. The logical

inconsistency of elastic rebound theory is obvious: how can elastic strain accumulate if the necessary medium continuity is already almost completely broken along a fault plane, particularly if the fault were pre-lubricated with graphite and/or pore-space fluids?

Thus, in the conventional plate tectonics-elastic rebound approach, the fault is illogically believed to be in a high potential critical state, via an absurdly contradictory process. The rise in that state is associated with a reduction of internal friction, which is a weakening process, i.e., if two bodies are decoupled to the degree that the friction coefficient approaches zero, continuity, and also elasticity, likewise approach zero, thus drastically reducing the elastic strain accumulation potential along the fault plane. So we must resolve this contradictory standard notion and give a reasonable explanation as to how an elastic potential rise can occur at all in fractured and incompetent rocks, and we must clarify what the source mechanism is for all earthquakes, e.g., shallow, deep, tectonic, or volcanic. In science we have to be logically consistent, concise, and precise, and we cannot constantly resort to ad-hoc illogical frameworks and convenient mental abstractions merely because they are long accepted and therefore widely popular.

Freund (2002, 2003), in his low-velocity and medium-velocity (~100 m/s to 5.64 km/s) impact experiments, demonstrated (a) A voltage rise of about 400 mV, about 200 μs after impact; (b) The coupling between the electron injection and the electric field at the rock surface, which resulted in damped oscillations with frequencies in the range of 8 to 45 kHz; (c) Charge carriers are generated locally by the impact and their quantity increases linearly with impact velocity, i.e., impact energy causes the rock to momentarily become highly conductive; (d) Such phenomena are not possible with rock samples under slowly increasing compressive or shear stress; a sudden stress load of an impact event is required; and (e) Heating is an infrared radiation. The implication of his experimental work is that rocks are plastic solids; the greater the impact energy, the greater the voltage rise, the higher the resonant frequency emitted will be; and there is, of course, no heat transferred by convection, which is redundant in an electromagnetically dominated Earth and upper mantle and crust.

The dramatic shortage and puniness of traditional Earth interior heat sources is shown in Table 3, which depicts the power per unit of mass provided by all possible radiogenic sources, and that actually required for the generation of a seismic or volcanic event. The traditionally allowed possible radiogenic sources can only provide less than 3×10^{-12} W/kg, but the energy concentration required for a seismic or volcanic event is in the range of 10^5 to 10^6 W/kg, or more than 17 orders of magnitude greater. In the context of EM, the ultimate source of internal energy is from compressed atomic orbital electron release during atom injection into the mantle and crust.

Thus, the source of thermal energy of Earth's interior is the radiant heat produced by these released resonating electrons inside the 10^{-6} to 10^{-5} m microfractures, which enable electrons to vibrate harmonically at thermal

frequencies, i.e., 5×10^{13} Hz. According to $E = hf$, where $h = 6.63 \times 10^{-34}$ J.s and $f = 5 \times 10^{13}$/s, each "new" electron can provide 3.3×10^{-20} J. About 4×10^{40} non-resonating electrons are required for the annual 1.3×10^{21} J of global heat loss. During resonance though, which occurs when about 10^7 "old" and "new" electrons surge harmonically within a resonant 10^{-6} m microcavity, the required quantity of electrons becomes much smaller, since in each resonant cavity, 10^7 electrons can provide 5×10^3 W of power. Power = ½ ($\rho_m \times \omega^2 \times z_o^2 \times v$), where $\rho_m = 10^{-23}$ kg/m, which is the mass density per meter of about 10^7 polarised and aligned electrons, per resonant cavity, in critical state conditions of frequency: $\omega = 2\pi f_1$ ($f_1 = 5 \times 10^{13}$/s); amplitude: $z_o = 10^{-5}$ m; force: $F = 10^{-7}$ N; and speed: v = (Force/Mass Density)$^{0.5} = 10^8$ m/s. Note that the power is proportional to the squares of both the amplitude and the frequency. By substituting, it comes out that the power delivered per resonant cavity (10^7 electrons) is 5000 W (J/s). Thus, just 8×10^{16} resonating electrons can supply the full 4×10^{13} W.

In all cases, for a seismic or lava melting-volcanic event, an intense spatial and temporal concentration of power is required. For example, if only this 4×10^{13} W of annual heat loss energy were readily available, in total, the maximum earthquake magnitude possible would be about 3, while an 8.9 seismic event requires a power of 10^{21} W.

As a resolution of the problem of energy-power concentration, we propose the following procedure: The ascent of EM atoms adds electrical charges, namely electrons and atoms, as effective semi-conductor p-holes. Electrons, having less mass, and being fast movers and more pervasive, are the first mobile charge carriers that manifest their differentiated electrical influence, by rushing into the smallest microcracks between crystals, the impedance of which is ~377 Ω, about four orders of magnitude lower than the resistance of 2.4 MΩ (resistivity, $\rho \cong 7500$ Ω.m) of granite (Freund, 2002). Once in the microcracks, their mutual electrostatic repulsion forces them to the microcrack-rock interface—exerting repulsive electromotive pressure (in volts) upon the electro-chemically bonded "walls" of the microcracks. Later, net positive charges are naturally attracted to the rock-microcrack interface, and, finally, the microcrack collapses as charge repulsion is cancelled out at discharge.

The microcrack collapse occurs when an increased concentration of electrons inside the microcrack, and/or of p-holes at the rock-microcrack interface, acting synergistically, suddenly drive the electrons outside the microcrack. Thus, microcracks, in effect, function similarly to directional flow-control valves, such as are designed to direct the flow of fluid, at a desired time and rate, to the location in a fluid power system, where it can be used to do mechanical work. In terms of an approximate mechanical metaphor, driving of a piston back and forth in its cylinder is an example of a directional control valve energy-flow application. Thus, microcracks are essentially "pressure-voltage"–operated devices, similar to n-p junction solid-state diodes. Electrons flow into the newly opening microcavities; if the directed pressure-EMF, related to the net

electron flow's polarity, is suitably coherently oriented as one, then the "valve" can open. As p-holes concentrate at the microcrack-rock interface, the net internal pressure-EMF "polarity" changes, the electron reservoir "flood-gate" opens, the electrons rush out and the transient microcavity collapses. At that point, "new" EM atoms and minerals form and are added and/or existing ones are altered, at the microcrack-rock interface, thus forming a new electrically neutral depletion region; then a new microcavity growth cycle can start if the ascent of EM from the core continues.

Provided that the total number of released electrons is above a critical threshold, the earthquake preparation process begins and completes with the generation of an earthquake, the magnitude of which depends on the size of the active volume. Otherwise, the action of the ascending EM and released "new" electrons is limited to thermal and other precursory effects, but no more. Thus, during the earthquake preparatory stage, EM Fe^{2-}, as electron "donors", convert into effective p-type, while Si^{4+} and $Fe^{2,3+}$ convert into effective n-type semiconductors, as they are flooded with newly released electrons from the ascending Fe^{2-}. So, quantified charge carriers flow toward the rock-microcavity interface, transforming the microcrack into an effective electrical capacitor, the dielectric, being "free-waveless" space itself, with characteristic impedance $Z_0 \cong; 377\ \Omega$, which at wave resonance velocities that tend to exceed light speed becomes an infinite impedance, signified by Z_∞. In other words, "free space" itself is the perfect elastic medium with actual inertial mass, exhibiting infinite impedance and instantaneous reflection of any excess elastic wave energy within it, i.e., of any wave tending to momentarily exceed light speed, the maximum deformation rate of elastic space itself. Reflective infinite impedance emerges at c, and thus prevents any elastic space wave from ever exceeding light speed. We call this real quantum "space", which pervades and forms the underlying basis of particle-wave–based matter, and also our finiteless cosmos, "Z_∞ Space"—paper to follow. This also shows us directly why light speed is the logical and natural absolute speed limit.

As the electromotive pressure inside the microcrack becomes too great, the impedance blocking discharge is attrited, and a dielectric breakdown, i.e., a transient discharging of the stored voltage, will cause a dramatic increase in local wave amplitude and a catastrophic, accelerating implosive collapse of the cavity, which is emptying its electrons. The greater the number of microcrack effective-capacitors connected in electrical parallel, the greater the capacitance of the total network and, therefore, the greater the potential EMF voltage difference stored.

Hence, we have to solve the following problem. How many excess electrons are required to produce a local electrostatic repulsion gradient that can actually overpower the "force" that holds atoms together? This traditional electromagnetic "force" is nothing other than the local tension gradient within an infinite, continuous, and perfectly elastic space itself, and in the forthcoming paper, we will present our detailed proposition of space, gravity, electromagnetic polarized

charges, and nuclear forces as literal elastic tension gradients within a perfect elastic Z_∞ Space—a singular ''force'', with scale-dependent expressions within a finiteless, continuous cosmos, in which all matter and energy are just variations upon how space itself ''waves'' elastically at its maximum deformation rate, c.

For separation and uplift to occur, the gravitational attraction and electrostatic repulsion have to be equal, $F_g = F_e = Gm_1m_0/r^2 = q_1q_0/4\pi\varepsilon_0 r^2$, then $Gm_1m_0 = q_1q_0/4\pi\varepsilon_0$ and $q_1q_0 = Gm_1m_0 4\pi\varepsilon_0$, as we have shown in the thought experiment (see Appendix).

The required amount of ''excess'' harmonically resonant electrons is in the range of $2 \times 10^{18}/m^2$, or $\sim 2 \times 10^6$ electrons per 10^{-6} m microcavity, which corresponds to a surface potential of about 3000 V and an electric field intensity gradient, across a flat surface, on the order of 3×10^9 Vm^{-1} a magnetic field gradient magnitude in the range of 10^2 T, a capacitance of 10^{-16} F per 10^{-12} m^2 microcavity, or 10^{-4} F/m^2. At the surface, ~33 km above, the corresponding current, electric, and magnetic field intensity changes will be on the order of 10 μA, 10 mV/m, and 10 nT, respectively.

The 2×10^{18} electrons/m^2 is seen to be a threshold number, a significant quantum quantity in physical geodynamical terms. At the depth of ~700 km, the maximum depth at which earthquakes occur, the required amount of electrons is three to four times higher. Thus, ~700 km marks the depth threshold at which the electron concentration becomes influential enough to cause uplift of the rocks above it. At greater depths, the electron repulsive force is less than the weight of the overlying material, so repulsive deformation cannot open microcrack cavities between crystals; hence, discharge of cavity electrons is non-existent and, thus, earthquakes will be non-existent below ~700 km depth in Earth.

Beyond this 2×10^{18} electrons/m^2 threshold, it is the amount of electrons flowing into the microcracks and the corresponding number of p-holes that later concentrate at the rock-microcrack interface that control and drive the process. When the necessary threshold EMF pressure is reached, electrical discharge occurs, resulting in the permanent gravitational collapse closure and sealing of the microcavity.

Figure 5 is a schematic representation of the dielectric establishment and breakdown process. At first, the injection of upward-moving electrons into a region of the mantle is impeded by a pre-existing net negatively charged electrical repulsion obstacle which halts upward movement of the electrons and causes them to accumulate below what becomes an effective electron ''dam''. The local EMF repulsion pressure gradient of these electrons increases internal microcrack pressure between rock crystals (black arrows), which overpowers overburden weight, or rather, gravitational attraction (white arrows). These newly forming microcavities occur along the electrical repulsive ''contact'' gradient with this obstacle to further upward ascent. This stage refers to the pre-earthquake quasi-stable energy storage period, in which the microcracks operate as resonant

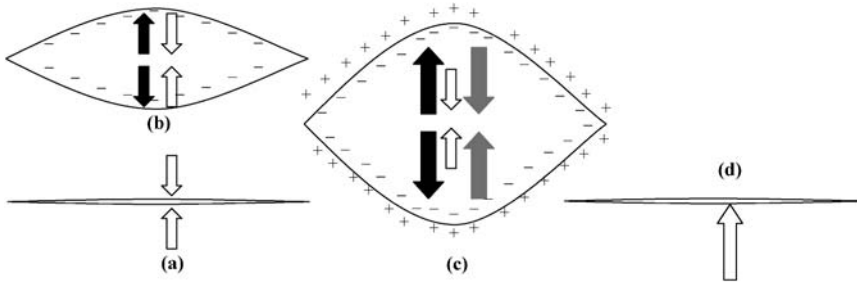

Fig. 5. Schematic representation of the dielectric breakdown cycle. The injection of electrons into a minute microcrack (a) increases internal pressure by increasing the electrostatic repulsion (black arrows), which locally overpowers gravitational attraction (white arrows). (b) As the number of electrons increases, the repulsive force also increases, thus resulting in the growing size of the microcrack and the high-pressure bulging-dilatancy of the locally tensional seismogenic volume. At about 90° out of phase, p-holes start to accumulate at the rock-microcrack cavity interface, and the attractive (grey arrows) neutralize the repulsive (black arrows) electrostatic forces, so that the only remaining force is gravitational attraction (c), leading to final gravitationally accelerating implosive collapse of the microcrack-effective-capacitor (d) and its return to almost zero volume (a).

cavities or wave traps, serving to concentrate and allow oscillation of ''old'' and ''new'' free electrons, at $\sim 10^{14}$ Hz, thereby releasing radiant infrared heat photon frequencies. As the number of electrons increases by one order of magnitude, e.g., to 2×10^{19} electrons/m^2, or $\sim 2 \times 10^7$ electrons per microcavity, the repulsive force, and therefore the size of the microcrack, also increases in tandem, from 10^{-6} to 10^{-5} m (Figure 5c). That translates to an electric field intensity in the order of 3×10^8 Vm^{-1}. This size increase of the microcrack is manifested by the pre-shock dilatancy-bulging of the seismogenic volume and by the reduction of the V_p/V_s velocity ratio (Feng, 1978). The measurable regional ground swelling-doming is a manifestation of electron storage near to Earth's surface prior to crustal depth earthquakes or prior to volcanism.

Also, later in time, p-holes start to accumulate at the rock-microcrack cavity interface, and, with a relative permittivity of 10, when the concentration of p-holes reaches $\sim 10^{20}$ p-holes/m^2 the attractive (grey arrows) neutralize the repulsive (black arrows) electrostatic force of $\sim 10^{19}$ electrons/m^2, so that the only remaining force is gravitational attraction (Figure 5c). Thus the dielectric collapse of the microcavities results to the gravitational collapse of the overburden rock mass (Figure 5d).

The apparent upward net direction of resulting compressional uplift is due to the greater mass and therefore inertial resistance to acceleration of the underlying material. As a result, the collapsing overlying mass is reflected back, and this observed predictable energy trajectory is manifested by the sharp downward first P wave motion, which is followed by an equally sharp upward motion, the amplitude of which is likewise predictably observed to be twice the displacement of the downward motion, thus indicating a lossless reflection of initial elastic shock deformational energy.

As we are treating the electron-filled microcavities as effective storage capacitors, let us recall the electrical properties of in-parallel and in-series conductively connected capacitors. Parallel connected capacitors always have the same voltage drop across any of them. They do not have the same charge unless they have the same capacitance, and the state within any one of them affects all of them electrically, directly and almost immediately. The capacitances and the charges add, while the effective resistance is the sum of their inverses, i.e., lower than the lowest individual resistance.

Conversely, all series connected capacitors share the same charge. The voltage storage potential of any individual capacitor depends on its dielectric's insulating properties, which act as an effective ''dam'', blocking electron discharge; but when the dielectric dam wall bursts, it fails and discharges totally, exponentially, and permanently. The effective capacitance, being the sum of their inverses, is lower than the value of any individual capacitor, whilst the voltages and resistances sum.

Since electricity and magnetism are actually one single equivalent phenomenon—electromagnetism—produced by their polarity difference interactions, we have to deal with the electrical property called ''reactance'', a critically important property of alternating currents and harmonically resonant wave systems. Reactance, X, is attributed to opposition to alternating current flow, resulting from inductance-magnetic field, X_L, and capacitance-electric field, X_C, that is $X = X_L - X_C$, and impedance, Z, is the total opposition to direct-resistance R, and alternating-reactance X, current flow in Amperes, as per $Z = (R^2 + X^2)^{1/2}$. There are two forms of reactance: ''inductive reactance'', concerning the magnetic field, and ''capacitive reactance'', concerning the electric field. These two reactances are opposite and will cancel/negate each other's influence in any harmonically resonant system, be it an antenna, an electrical circuit, or an electron-filled 10^{-6} m resonant cavity.

Inductive reactance is associated with the varying magnetic field that surrounds a current, $X_L = 2\pi fL$, where f is the resonant frequency in Hertz (Hz) and L is the inductance in Henry (H); therefore, a varying current is accompanied by a varying magnetic field gradient in space; the latter gives an EMF gradient which resists the changes in current flow. As with elasticity and plasicity that increase in tandem, the more the current gradient changes, the more an inductor's magnetic gradient resists it. Therefore, the reactance oscillation is proportional with the tuned resonant frequency, and tends toward zero for direct current and toward infinity for alternating current. Similarly, for constant resonant frequency, as the inductance of a component increases, its inductive reactance becomes larger in imaginary terms. There is also a phase difference between the current and the applied voltage, which is, of course, naturally mirrored in Freund's experiments.

On the other hand, capacitive reactance, $X_C = 1/(2\pi fC)$, is associated with the changing electric field between two conducting surfaces, separated from each other by a dielectric insulating medium, where f is the resonant frequency in Hz

and C is the capacitance in Farad (F), and this equation reflects the fact that electrons, when travelling as a direct current (DC), cannot pass. But effectively, an alternating current can pass the dielectric, and as the value of capacitance or resonant frequency increases, the opposition to the flow of alternating current decreases, and its capacitive reactance approaches zero in imaginary terms. There is also a phase difference between the alternating current effectively flowing through a capacitor and the DC potential difference across the capacitor.

The most important thing to remember about these two reactances is that in order to electronically harmonically resonate a given wave frequency, in any physical electrical system, these two reactances must be balanced so that both are precisely equal but opposite in value at the desired resonating frequency. Unless these reactances are balanced at the physical length of the system, self-organising polarised electron resonance within the parallel microcrack network cannot occur.

In our case, each 10^{-5} m microcavity effective-capacitor has a charge of 0.32 C, a voltage of 3000 V, and a capacitance of 10^{-16} F. Let us now examine 10^5 cavities connected in parallel and 10^5 connected in series. Since the net electron flow over time is toward Earth's surface, the in-parallel microcavities line up (polarise) horizontally, while the in-series cavities are piled up vertically. Therefore, the logistics are the following; In the 10^5 in-parallel connected microcavities the voltage drop is 3000 V, the charge is $10^5 \times 0.32 = 3.2 \times 10^4$ C, and their capacitance is $10^5 \times 10^{-16}$ F $= 10^{-11}$ F. However, the 10^5 vertically piled up microcavities will result to an uplift of 1 m, the charge on the equivalent capacitor is 0.32 C, the voltage drop is 3×10^8 V, and the capacitance will be only 10^{-21} F.

In other words, as shown in Figure 6, in the in-series connected microcavity effective-capacitors (grey), the capacitive reactance will have its maximum, i.e., becomes smaller in negative imaginary values (closer to zero), and the inductive reactance has its minimum positive imaginary number value, i.e., approaching zero from the opposite direction. The opposite occurs in the in-parallel conection, but in both cases, when the sum is zero at the resonant wavelength of the system, current becomes direct, i.e., moving with constant speed on straight lines. In that circumstance, the conductively networked microcrack cavity electrons will very suddenly polarise as one, strongly resonating with high efficency at the cavities' harmonic resonant tuned frequency. The network's amplitude will suddenly exponentially reach peak focused polarised amplitude and EMF pressure maximum, leading to tuned discharge/transmision of the electrons out of the cavities, generally toward Earth's surface, as a polarised, localised, and therefore extremely concentrated high-ampere EMF energy flow. This electron transmission is the determining mechanism of magma formation and earthquake generation.

The implication in Figure 6 is that collapse, after post-discharge cavity implosion, will start at the central higher part of the network and can continue in a similar fashion, when and where equal but opposite electronic inductive and capacitive reactances intersect and cancel each other out, inducing cavity electron resonance and photon emission at $\sim 10^{14}$ Hz, and at 45° relative to the

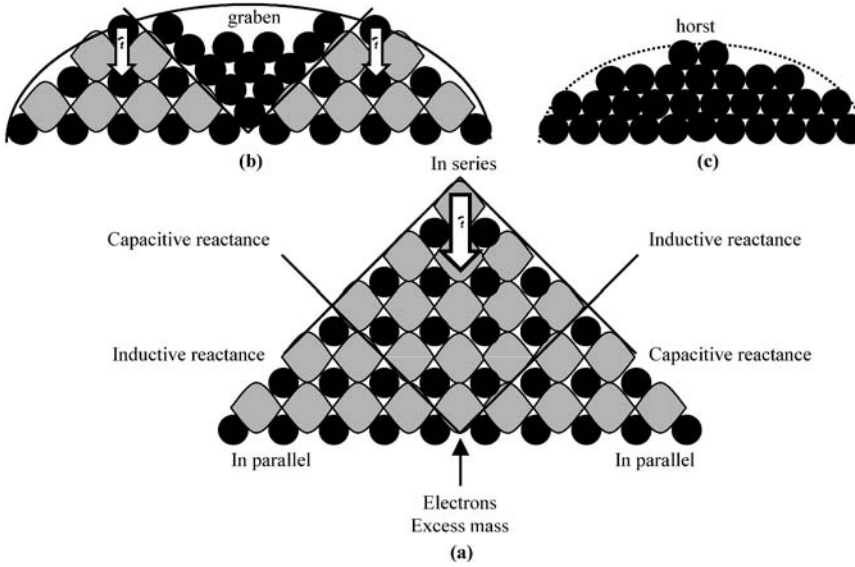

Fig. 6. In series, connected microcavities (grey) pile up vertically, while the in-parallel ones line up horizontally. The space in between the microcavities is filled with ''new'' excess mass atoms (black cycles). In the in-series connected microcavities, capacitive reactance will have its maximum negative and inductive reactance its minimum positive imaginary values. Conversely, the capacitive reactance will reach its minimum and inductive reactance its maximum in the in-parallel connection (a). The collapse, if and when equal but opposite electronic inductive and capacitive reactances intersect, so cancelling each other out at the tuned resonant harmonic frequency of $\sim 10^{14}$ Hz, will start at the central highest area. The result will be a domed net uplift of rocks above (dotted line), possibly with the formation of a graben (b) or a horst (c), if the entire active volume collapses as a single network.

vertical and horizontal axis. The result will be a dome at Earth's surface (dotted line), the net height of which will be less than the initial pre-shock uplift achieved. That the dome is an aftershock structure is attributed partly to the failure of part of the microcavity network, and partly to the filling of the space in between the microcavities with ''new'' excess mass atoms (black circles), which are the result of opposite charge ''neutralization''. The eventual residual resonance of other parts of the network produces aftershocks for days, weeks, and months after the primary resonance event, and in some cases, even as warning precursors to the main shock. If the volume of the EM is less than the volume that has collapsed, a graben topography will form in its central part (Figure 6b). Conversely, if the upper threshold is exceeded in the entire active volume, a horst topography will likely develop (Figure 6c).

How then do our theorizations correspond to the natural world? A high-energy impact, in which most of the impact's energy is used to do the mechanical work needed to overcome the normal inter-atomic electromagnetic forces that keep atoms of a crystalline unit cell in place, i.e., frictional energy, can cause a plastic

solid to deform momentarily, as if it were genuinely a true and highly deformable elastic substance. If the shear stress is greater than about 10^8 Pa, or the strength is greatly reduced, a fault can form. A fault can have a surface manifestation, or it can be exhumed by erosion and subsequent long-term uplift, or else it can remain permanently buried. Being a zone of weakness in the rock, it can rupture and move again more easily after a strong shock than a more continuous and competent nearby rock mass.

Lubrication of a fault is simply not necessary at the energies involved, though a lubricated boundary layer will of course move preferentially, so that it appears, superficially at least, that lubrication was a significant active factor. But actually, it is only a minor secondary geodynamic factor in deciding what moves where, and by how far. Certainly lubrication of a fault is not any sort of determining control on whether the regional earthquake shock movement occurred at all. Resonance timing and scale are the primary controls in all earthquakes.

The elasticity activation energy is magnitude independent, so seismic efficiency, that is, the ratio of radiated seismic wave energy, E_R, over total energy-seismic moment, M_0, should depend on potential, and it will tend to be lower for smaller and higher for larger events. Indeed, for large earthquakes ($M > 5$), the E_R/M_0 is in the order of 10^{-4}, while for small events ($M < 2.5$) it can be as low as 10^{-7} (Kanamori & Brodsky, 2001), i.e., greater force per unit area, and therefore greater efficiency, and this fact is observed in deep earthquakes. This logic is also confirmed experimentally (Freund, 2003). Low-velocity impacts, at ~100 m/s, activated p-hole charge carriers only in a small volume near the impact point, while the medium velocity impact of ~1.45 km/s had enough energy to activate the p-holes in the entire rock volume of 0.0125 m^3. In other words, the greater the stress and imparted energy, the greater the rigidity and therefore the elasticity of the impacted medium, which acquires an infinite value if "free space" is bombarded at light speed, i.e., all of the energy will be reflected back.

Let us now take the 7.4 Izmit earthquake, about which reliable high-tech data exist (Figure 7). Satellite interferometry indicates an aftershock elliptical dome measuring 250 km × 60 km × 75 cm, i.e., a spherical segment of an area $\sim 1.2 \times 10^{10}$ m^2, uplifted by about 75 cm; thus, the active volume and the active mass—actually the EM—are in the range of 4.4×10^9 m^3 and 1.3×10^{13} kg, respectively.

The focal depth of the Izmit earthquake was 17 km (U.S. Geological Survey). Therefore, the deformed volume was ($\sim 1.2 \times 10^{10}$ $m^2 \times 17 \times 10^3$ m =) $\sim 2 \times 10^{14}$ m^3, which corresponds to a mass of about 6×10^{17} kg. If that mass is elevated and then allowed to collapse, as in free fall, from an average height of 83 cm, in about 0.4 s, and at a velocity of ~4 m/s, which is more than 10 orders of magnitude greater than the few cm/yr of the supposed plate motion, it can provide the power of 5×10^{18} W for the 7.4 earthquake. The 6×10^{17} kg of mass represents a total force of 6×10^{18} N, or a static stress of $\sim 5 \times 10^8$ Pa, which is enough to break intact rock. The 5×10^{18} W of power, if multiplied by the ~20 seconds of source duration (Bock, 2000), can supply the $\sim 10^{20}$ N.m of the Izmit earthquake. The pre-shock uplift should be higher than the net aftershock one,

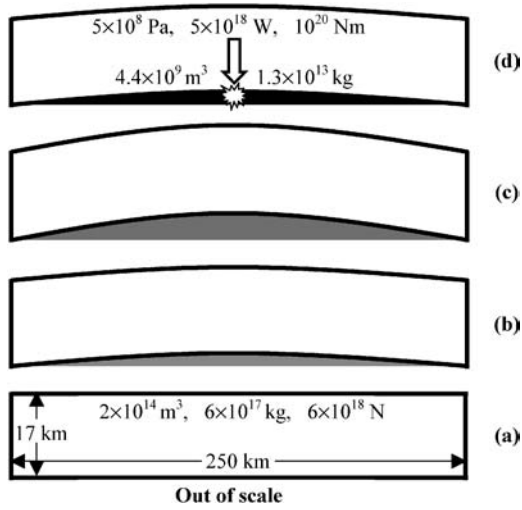

Fig. 7. The physics of the source of the 7.4 Izmit earthquake, h =17 km. Satellite inteferometry data indicate a post-seismic elliptical dome 250 km × 60 km × 75 cm, i.e., a spherical segment of volume $\sim 4.4 \times 10^9$ m^3 and mass $\sim 1.3 \times 10^{13}$ kg (black lens), i.e., active volume and active mass, respectively. The deformed volume of $\sim 2 \times 10^{14}$ m^3 that corresponds to a mass of $\sim 6 \times 10^{17}$ kg and a force of $\sim 6 \times 10^{18}$ N (a) was uplifted, due to pre-seismic microfragmentation (light gray lens) (b), enlargement of microcracks, and addition of excess mass (dark gray lens) (c). At dielectric breakdown, the elevated volume-mass collapsed from a height of ~83 cm (d) and provided the stress of $\sim 5 \times 10^8$ Pa, at a rate of ~4 m/s, the power of $\sim 5 \times 10^{18}$ W, and the $\sim 10^{20}$ N.m of seismic moment that are required for the generation of the 7.4 shock. The net 75 cm high aftershock dome (black lens) is the manifestation of excess mass transferred upward from Earth's core.

due to both excess volume-microcavities collapsing and EM rise, so the net 75 cm high dome is a manifestation mainly of EM addition to the crust.

Correspondingly, for the 5.9 (September 7, 1999) Athens earthquake, with 17 km focal depth (Papadopoulos *et al.,* 2000), an area in the range of $\sim 2 \times 10^9$ m^2 (r = ~25 km), or a mass of $\sim 10^{17}$ kg, needs to be uplifted by ~20 cm in order to supply the $\sim 2 \times 10^{17}$ W, which, if multiplied by the 5 seconds of source duration (Papadimitriou *et al.,* 2000), can provide the 10^{18} N.m of its seismic moment.

As negative EMF charge pressure builds up within the microcrack electron-storage cavities, the EMF potential gradient exceeds the effective reverse bias diode-like impedance barrier, and the vertically polarised resonating electrons rush out of the microcrack as they effectively ''earth'' toward a location of lower EMF pressure gradient, i.e., to a region of much lower voltage. The catastrophic cavity network collapse which follows discharge is similar to dielectric breakdown and failure of a capacitor. The drop of geoelectric potential and the increased conductivity at the earthquake preparatory stage, that observably culminates co-seismically (Noritomi, 1978; Wang, 1978), corroborates the logic presented here, that an earthquake itself is fundamentally an electromagnetic phenomenon. Thus, the same processes that are responsible for the pre-shock

electromagnetic phenomena can, but don't necessarily have to, conclude with the generation of an earthquake shock.

In the context of a solid discrete quantum threshold controlled geochemical Earth, reduced iron (Fe^{2-}) acting as an electron ''donor'', converts Si^{4+} and $Fe^{2,3+}$ into an effective charged n-type semi-conductor and itself into an effective positive net charge p-type semiconductor. The electromotive pressure potential difference maximum is in a line directly between them. Therefore, the cause is the flooding or ''doping'' of silicate and iron oxide minerals with excess electrons-plasma, released from the ascending Fe^{2-}, which then becomes an effective p-hole. Electrons, being much less massive and traveling at far greater average speeds, will follow the least EMF pressure potential difference and also kinetic resistance path, at all times, and enter into the smallest spaces or cracks between crystals, enlarge them, and vibrate within at thermal frequencies, thus releasing radiant heat and some slow conductive heating as a result. Implicit in this is that near-surface heating occurs where large numbers of electrons are present, and the hottest observed regions will also be associated with higher seismic potential and dynamic geological phenomena. Concurrent with the formation of microcracks from rising EMF repulsive gradients, the produced sound waves can initiate a new out-of-phase cycle, in which the formation of p-holes precedes, and electric current follows, in response to their creation and change of the potential gradient, as Freund (2002, 2003) and Freund *et al*. (1993) have experimentally shown as well.

Similarly, it is these same excess electrons, in a ''cold'' environment, which result in the orders of magnitude enhancement of the effective electrical conductivity of olivine crystals, which is confined to crystal surface flow, but disappears at temperatures above 700°C (Constable & Duba, 1990).

Provided that excess electrons, donated by decompressing iron shells, arrive at the surface from within the mantle and outer core, the EMF potential gradient flux recovers strength, microcavities can redevelop, and a fresh earthquake preparatory cycle can begin, with the slow charging of new microcavities with rising electrons. But, when the supply of ''new'' electrons is reduced to values below the EMF level that can cause the discharge and collapse of the microcavities, the frequency of the oscillations decreases. Eventually the whole process stalls or becomes dormant when the number of excess electrons remains below the quantified threshold of $2 \times 10^{18}/m^2$ of electrons in rocks.

In his experimental work, Freund (2002, 2003) also has shown that ''... P and S waves had died down within about 200 μsec after impact ...'', thus giving merit to the notion that rocks are plastic solids but can respond momentarily elastically if they receive a high stress rate impact—in his experiment, a medium-velocity bullet impacts at 1.46 to 5.64 km/s—and after that, the rocks return to their plastic solid state. If the impact rate is below a certain very low threshold, there will be no elastic response at all, and if this threshold is exceeded, the proportionally generated seismic waves will travel with velocities

on the order of kilometers per second, the velocity depending on the elastic properties of the rock medium. In nature, during the critical conditions of dielectric breakdown, almost all the energy is used to produce transient mechanical work, and the high stress rate coerces the plastic rock to respond instantaneously like a quivering elastic gel, rather than a rock.

What then determines an earthquake's magnitude is the average density of microcrack resonant cavities, i.e., the electron density for a given rock volume, or else, a greater volume for a constant density of microcracks, but ultimately, it is the quantity of EM injected from below, and the resulting excess electrons, inducing an intense, contained, localised repulsive EMF pressure gradient. Therefore, if the supply of excess electrons continues, a new electromagnetic thermal and earthquake preparatory cycle will progress.

In strong earthquakes, the amount of heat released is estimated to be in the order of 10^{18} J (Kanamori & Brodsky, 2001), which is comparable to the thermal energy released during large volcanic eruptions. Heat, as ''hidden'' vibrational energy, can cause melting to a few centimeter thick layer over the whole extent of the affected microcavity volume, and secondarily, along faults that may or may not form, due to intense mechanical friction of the sudden slippage. Moreover, the absence of short-period waves, which, if present, are indicative of fault surfaces rubbing against each other, is another strong piece of evidence against elastic motivation of fault planes. In other words, shock-related thermal energy accumulation is mainly due to both kinetic impact of cavities slamming closed and to the kinetic action of escaping electrons accelerating and thereby thermally vibrating.

Thus, T. F. Freund's p-holes not only provide a unified insight which neatly explains earthquake-related electric, electromagnetic, and luminous non-seismic precursory phenomena, e.g., resistivity changes, ground potentials, earthquake lights, etc., but can also be seen as a crucial, integral aspect of the earthquake generation process and of geodynamics in general.

The Earthquake Prediction Issue

In the EM conceptual framework, the earthquake nucleation process is considered as an Electro-Magnetic Self-Organized Criticality (EMSOC), in which the earthquake preparatory process starts when the lower threshold of $\sim 10^{18}$ electrons/m^2 is surpassed, but an earthquake occurs if and when the contained local EMF pressure gradient becomes sufficiently amplified during cavity resonance of electrons and p-hole concentration at the rock-microcrack interface. Between the lower and the upper threshold, e.g. $>10^{19}$ electrons and/or p-holes/m^2, resonating ''new'' and ''old'' free electrons at $\sim 10^{14}$ Hz within the 10^{-6} to 10^{-5} m microcavities release radiant heat and, later, local kinetic resistive heating during ''arcing'' to lower potential difference regions. When the necessary upper threshold is reached and the size of the cavity and its resulting wavelength increase, the network of sympathetically resonating cavities empties

and collapses in harmonic unison, producing an adiabatic elastic reflective "bounce" response. In that context, solid Earth tides can trigger earthquakes by widening microcracks, thus facilitating the entrance of electrons into them and accelerating the process of earthquake nucleation.

In China during the period from 1975 to 1976, there was a clustering of 10 major earthquakes with magnitudes from 6.7 to 7.8. Some of them were predicted, and among them, the Haicheng 7.3 earthquake on February 4, 1975, which is the only known successful imminent earthquake prediction that led to the evacuation of a city a few hours before the shock. But, the Tangshan 7.8 earthquake, on July 28, 1976, had no foreshock activity, and it was not predicted. In all cases, the seismic characteristics, e.g., foreshocks, or non-seismic precursors, were different (Oike, 1978). Also, in China, 30 false alarms in three years were issued (Main, 1999). Clearly, indeterminacy is inherent with earthquakes, and the use of deterministic methods, especially for imminent earthquake prediction, is unjustifiable (Geller, 1997).

Therefore, there are two uncertainties, and their implications need to be taken into consideration: the upper threshold and the size of the active volume. The implications of the lower and upper threshold uncertainties are these:

1) You may have a flux of thermal and volcanic processes, as well as earthquake precursors, for a considerable length of time, which are not followed by a minor or major earthquake. The upper threshold is "never" surpassed, and therefore, an earthquake is not generated.
2) A very quick surpass of the lower and the upper thresholds, and therefore the rapid progression of the earthquake preparatory stage, is immediately followed by the generation of a minor or a major shock. Precursory potential warning phenomena will be practically absent.
3) There is a "reasonable" time duration between surpassing of the lower and the upper thresholds and, therefore, between precursory phenomena and the generation of an earthquake.

Since the magnitude of an earthquake depends on the size of the active volume, additionally, we have to consider the size of the active volume uncertainty, which means:

1) Ideally, the upper threshold is exceeded at first in several small adjacent active volumes, later as a co-joined network in a larger one, and soon after, in many residual smaller adjacent volumes. In conventional terms, this is a "*regular*" earthquake sequence, with a sprinkling of *foreshocks*, a *main shock*, and many, progressively fewer *aftershocks*.
2) Actually, the upper thresholds are exceeded in many small neighboring volumes in a very short period of time or, in bigger ones, further apart in space and time, i.e., the greater the magnitude, the greater the implied apparent spatial and temporal dispersion of threshold crossing. This is a typical case of earthquake clustering, or seismic *swarm*, whereby no

earthquake has a distinctly higher magnitude. Given the relativity of space and time, you might have all sorts of spatial and temporal variations. In other words, each earthquake is an independent and stochastic event—even when tightly clustered in time and space, they still remain quite unpredictable in timing, focal location, or magnitude.

3) The upper threshold is exceeded at first in some small volumes, later in a larger one, and the underlying deep-seated energy phenomenon stalls. Some foreshocks and a main shock, but no aftershocks, occur.
4) The upper threshold is exceeded, at first in a large volume, and soon after in smaller volumes. This is an often-encountered case, whereby a main shock is not preceded by any foreshocks, but is followed by up to years of aftershocks.

Thus, a reasonable mechanism is also offered as to why precursory electromagnetic phenomena are not always followed by an earthquake; this mechanism also explains the haphazard variable duration, from seconds to years, of the precursory stage to when an earthquake finally triggers (Biagi, 1999; Bowan & Sammis, 1999). We see and measure the random seismic tip of an uncooperative hidden iceberg, whose actual submerged extent, dynamics, and shape we cannot accurately measure or predict.

The Macro-Scale

The above is our proposition concerning the micro-scale of Earth's interior. What then of the macro-scale implications? Observation shows that earthquakes and associated phenomena, such as volcanism, spatially cluster at the boundary between mobile, stable, positive and negative gravity anomaly regions, in island arcs, in intra-continental areas, and in mid-ocean ridge settings, at the global, regional, and local scales as schematically depicted in Figure 8. Thus, earthquakes concentrate toward low-altitude, low-gravity areas, while high-gravity zones tend to have fewer earthquakes and more volcanoes and, hence, higher heat flow rates (Kulinich *et al*., 2000; Maslov, 1999).

NASA's latest geophysical-gravity satellite is GRACE (Gravity Recovery and Climate Experiment), launched on March 17, 2002; GRACE uses microwave signals to determine very precisely the vertical distance between spacecraft and points on the ocean and land surface, to obtain dynamic sea surface height data, which is three orders of magnitude more precise than previous data. This yields a much more detailed picture of Earth's geoid, or mean gravity field distribution. In July 2003, the GRACE team released the most accurate gravity map yet of the entire planet, and this map shows dynamic variations down to the centimeter level. A correlation comparison of this global gravity map with seismicity and active volcanism geography clearly depicts that the high-gravity circum-Pacific Ring of Fire associates strongly with active volcanoes, and seismic activity concentrates at the distinct petrologic anisotropic boundaries, between high- and low-gravity regions.

Also, according to U.S. Geological Survey data, the earthquakes of magnitude 6 or greater, since 1868 on the Island of Hawaii, occurred at the flanks of Mauna Loa, Kilauea, Mauna Kea, and Hualalai volcanoes.

Earthquakes require anisotropy, and anisotropy exists at physical and chemical boundaries. The contact zone between a mobile stress-fractured region and a stable consolidated region is one such boundary. The two regimes are different kinematically, i.e., one is rising and the other is immobile. Geotectonically significant anisotropies can also be chemically and mineralogically defined, such as a discrete ocean crust and continental crust juncture, since the static old mineral regime is made of felsic minerals and rocks, i.e., rich in K, Na; while in the rising new mafic mineral regime, Fe and Mg dominate silicates. On the other hand, volcanism generally often occurs in relative isotropic settings. Volcanism is the outcome of earlier microcrack formation; these microcracks then serve as resonant cavity networks which form asthenolenses (Pratt, 2000), i.e., lens-like seismic wave low velocity zones.

Conclusions

1. Remnant primordial heat, tidal heat, and decay of radioactive elements are pathetically inadequate to provide heat energy for thermally driven geodynamic processes. On the contrary, localised natural electromagnetic anisotropic concentration processes can easily supply and deliver the energy required to drive Earth's observed geodynamics.
2. In direct contradiction to plate tectonics theorizations, global seismic tomography data indicate that horizontal movement of decoupled, or even coupled, ''lithospheric'' plates is not occurring, and subduction is physically irreconcilable and profoundly implausible.
3. The high Q value, i.e., the remarkably low attenuation-friction state of the outer core, and its attenuation of S waves, indicate that Earth's core is a highly conductive, low ambient temperature, high-frequency/energy, highly ''fluid'', and therefore a quantum threshold, rather than a thermal dynamics–controlled environment.
4. Elastic moduli and velocity of both P and S seismic waves increase sympathetically with growing depth inside the Earth's mantle. The natural implication of a rigid solid, cold, and non-convecting, almost immobile rock mantle is both inescapable and contiguously logical.
5. The crust, being micro- and macro-fragmented, is the most discontinuous and therefore most inelastic medium of the Earth's solid parts and is incompatible with high elastic strain storage.
6. Supposed plate motions and static stress changes along faults cannot generate nor trigger earthquakes, but a sudden stress load can produce both earthquakes and occasionally fault ruptures.
7. Earthquakes cluster in space and time. They tend to concentrate at the mechanically and chemically anisotropic boundaries between mobile

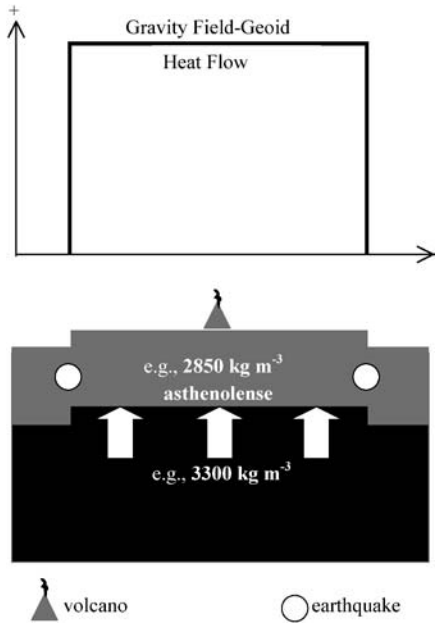

Fig. 8. Mobile belts in island arcs and in intra-continental regions associate with seismicity, volcanism, tectonism, high heat flow, and positive gravity anomalies, all of which are manifestations of ascending excess mass atoms and electrons. Earthquakes occur at the more anisotropic boundaries, between mobile and stable regions. Due to such anisotropy, earthquakes are naturally more likely to occur at the boundary between low- (basins) and high (uplifted)- gravity areas. High-gravity zones in active regions tend to have fewer earthquakes but an affinity with volcanic activity.

and stable regions, while volcanoes tend to concentrate in high-gravity areas.

8. The energy concentration for either a volcanic or seismic event is in the range of 10^6 W/kg, about 18 orders of magnitude greater than the $<3 \times 10^{-12}$ W/kg radiogenic sources could optimally possibly provide.
9. EM produced in the outer core, through a natural, predictable material plasma transformation process, is electromagnetically pressure injection added to a tensioned mantle and crust in the form of solid-state ''wedges'', and geodynamic energy is transferred from core to surface as compressed electron orbitals of Fe^{2-}.
10. Anisotropy is a ''sine qua non'' prerequisite of seismogenesis. Structural and/or physical discontinuities or obstacles at a boundary zone between the ascending-mafic and static country rocks, which can be either felsic or mafic, impede the ascent of Fe^{2-} and other atoms, forcing them to accumulate in situ, releasing and flooding the rock volume with their decompressing outer orbital electrons, which open, widen, and then inhabit local 10^{-6} m microfractures.

11. At $\sim 10^{18}$ electrons/m^2 density, microcracks form, enlarge, and consequently act as natural resonant cavities for free electrons which radiate at $\sim 10^{14}$ Hz, the radiant heat infrared part of the electromagnetic spectrum. This mechanism drives heating and the full gamut of volcanic and associated metamorphic, hydrothermal alteration, and mineralisation processes.
12. Microcracks act as effective electrical energy-storage capacitors (volts), connected in parallel. An earthquake occurs if and when the local concentration of electrons and p-holes, acting synergistically, increase the EMF gradient to uncontainable pressure levels. The resulting dynamic change in electrical potential gradients then drives the electrons out of the microcavities, which thereafter immediately collapse, due to the immense overburden weight and static pressure. The implosive coming together of their walls produces an adiabatic reflective elastic ''bounce'' stress rate that then generates the seismic waves of any earthquake.
13. The earthquake's magnitude depends on the volume and density of electron-filled microcavities in the active volume, i.e., in which the upper electron density threshold is surpassed.
14. An earthquake is effectively a stochastic phenomenon, and the use of deterministic methods in earthquake prediction is unwarranted.
15. The ultimate implication of this EM geodynamic framework is that physical finiteness itself does not exist in any physically ultimate sense. Material infinity is therefore the only possible and useful physical condition from which to comprehend observations and to derive their logical implications and significance. But, Socrates was right, after all: we know nothing; because how can you understand and express with abstract and limited ideas the unlimited and material actual?

Acknowledgments

Science, in short, regards the comprehensible implications of observations and logic, and its progression implicitly requires direct honesty and, certainly, controversy. In that context, we are sincerely grateful to Prof. Karsten Storetvedt and Dr. Chris Smoot for critically reviewing the initial manuscript. Their constructive critiques and insightful and detailed remarks helped us to avoid ambiguity and stick to the facts, and their logical implications. Certainly we do not submit to some critique, particularly those concerning the question of global expansion, but it would require another long paper to present our detailed arguments regarding Earth expansion within a steady-state cosmos. We reserve the right to do so in a future paper.

References

Aki, K. (1966). Generation and propagation of G waves from the Niigata earthquake of June 16, 1964: Part 2. Estimation of earthquake moment, released energy and stress drop from the G wave spectra. *Bulletin of the Earthquake Research Institute, University of Tokyo, 44,* 73–88.

Bak, P., & Sneppen, K. (1993). Punctuated equilibrium and criticality in a simple model of evolution. *Phys. Rev. Letters, 71,* 4083–4086.
Beloussov, V. V. (1980). *Geotectonics.* Moscow: Mir Publications.
Biagi, F. (1999). On the existence and complexity of empirical precursors. *Nature, Debate on Earthquake Prediction,* 18 March 1999.
Bock, G. (2000). Rapid Source Parameter Determination of the August 17, 1999, Izmit Earthquake at GFZ Potsdam. *ORFEUS Newsletter, 2,* 3.
Bolt, B. (1976). *Nuclear Explosions and Earthquakes: The Parted Veil.* W. H. Freeman.
Bolt, B. (1982). *Inside the Earth.* W.H. Freeman.
Bowam, D., & Sammis, C. (1999). A case for intermediate-term earthquake prediction: Don't throw the baby out with the bath water! *Nature, Debate on Earthquake Prediction,* 18 March 1999.
Chang, W. Y., & Zhong, J. Y. (1977). On the development of fracture-systems in China. *Science of Geology Sinica,* 197–209 (in Chinese with English abstract).
Constable, S., & Duba, A. (1990). Electrical conductivity of olivine, a dunite and the mantle. *Journal of Geophysical Research, 95,* 6967–6978.
Crisp, J. (1984). Rates of magma emplacement and volcanic output. *Journal of Volcanology and Geothermal Research, 20,* 177–211.
Dziewonski, A. M., & Anderson, D. L. (1981). Preliminary Reference Earth Model. *Physics of the Earth Planetary Interiors, 25,* 297–356.
Ernst, R. E., Grosfils, E. B., & Mege, D. (2001). Giant dike swarms: Earth, Venus and Mars. *Annual Review of Earth Planetary Sciences, 29,* 489.
Feng, Te-yi. (1978). Anomalies of seismic velocity ratio before the Yongshan Daguan earthquake (M=7.1) on May 11, 1974. In *Chinese Geophysics* (pp. 47–53). American Geophysical Union.
Freund, F. (2002). Charge generation and propagation in rocks. *Journal of Geodynamics, 33,* 545–572.
Freund, F. (2003). Rocks that crackle and sparkle and glow: Strange pre-earthquake phenomena. *Journal of Scientific Exporation, 17,* 37–71.
Freund, F., Freund, M. M., & Batllo, F. (1993). Critical review of electrical conductivity measurements and charge distribution analysis of MgO. *Journal of Geophysical Research, 98,* 22209–22229.
Geller, R. J. (1997). Earthquake prediction: A critical review. *Geophysics Journal International, 131,* 425–450.
Grand, S. P. (1987). Tomographic inversion for shear velocity beneath the North American plate. *Journal of Geophysical Research, 92,* 14065–14090.
Grand, S. P., Van der Hilst, R. D., & Widiyantoro, S. (1997). Global seismic tomography: A snapshot of convection in the Earth. *GSA Today, 7,* 1–7.
Hanssen, R., Vermeersen, B., Scharroo, R., Kampes, B., Usai, S., Ruediger, G., & Klees, R. (1999). Deformation pattern of the 17 August 1999, Turkey earthquake observed by satellite radar interferometry. Delft Institute for Earth-Oriented Space Research (DEOS), Delft University of Technology.
Ito, K. (1995). Punctuated equilibrium model of evolution is also an SOC model of earthquakes. *Physical Review E, 52,* 3232–3233.
Jackson, D. D. (1999). The status of earthquake prediction. *Nature, Debate on Earthquake Prediction,* 18 March 1999.
Kagan, Y. Y., & Jackson, D. D. (1991). Long-term earthquake clustering. *Geophysics Journal International, 104,* 117–133.
Kanamori, H., & Brodsky, E. E. (2001). The physics of earthquakes. *Physics Today, 54*(6), 34–40.
King, G. C. P., Stein, R. S., & Lin, J. (1994). Static stress changes and the triggering of earthquakes. *Bulletin Seismological Society of America, 84,* 935–953.
Knopoff, L. (1999). Earthquake prediction is difficult but not impossible. *Nature, Debate on Earthquake Prediction,* 11 March 1999.
Kulinich, R. G., Maslov, L. A., Gilmanova, G. Z., & Komova, O. S. (2000). Density model and crustal stresses in Northern part of Sea of Japan. *Geology of the Pacific Ocean, 15,* 391–404.
Main, I. (1999). Is the reliable prediction of individual earthquakes a realistic scientific goal? *Nature, Debate on Earthquake Prediction,* 25 February 1999.
Maslov, L. A. (1999). Simple model for computing crustal and lithospheric stresses and its interpretation results. *Geology of the Pacific Ocean, 14,* 227–242.
Noritomi, K. (1978). Application of precursory geoelectric and geomagnetic phenomena to earthquake prediction in China. In *Chinese Geophysics* (pp. 377–391). American Geophysical Union.

Oike, K. (1978). Precursory phenomena and prediction of recent large earthquakes in China. In *Chinese Geophysics* (pp. 179–199). American Geophysical Union.
Papadimitriou, P., Kaviris, G., Voulgaris, N., Kassaras, I., Delibasis, N., & Makropoulos, K. (2000). The September 7, 1999 Athens earthquake sequence recorded by the Cornet Network: preliminary results of source parameters determination of the mainshock. *Annales Geologiques des Pays Helleniques, 38,* 29–40.
Papadopoulos, G. A., Drakatos, G., Papanastasiou, D., Kalogeras, I., & Stavrakakis, G. (2000). Preliminary results about the catastrophic earthquake of 7 September 1999 in Athens, Greece. *Seismological Research Letters, 71,* 318–329.
Pollack, H. N., Hurter, S. J., & Jonhson, J. R. (1993). Heat flow from the Earth's interior: Analysis of the Global Data Set. *Reviews of Geophysics, 31,* 267–280.
Pratt, D. (2000). Plate tectonics: A paradigm under threat. *Journal of Scientific Exploration, 14,* 307–352.
Press, F., & Siever, R. (1978). *Earth*. Freeman.
Shih, Chen-liang, Huan, Wen-lin, Yao, Kuo-Kann, & Hsie, Yuan-ting. (1978). On the fracture zones of the Changma earthquake of 1932 and their genesis. In *Chinese Geophysics* (pp. 17–45). American Geophysical Union.
Smoot, C. N. (2002). Ubiquitous megatrends obfuscate seafloor spreading concept. In *Proceedings of the International Symposium on NCGT*, May 2002, Otero Junior College, La Junta, CO, 1–35.
Sornette, D. (1999). Earthquakes: From chemical alteration to mechanical rupture. *Physics Reports, 313*(5), 238–292. Available at: http://xxx.lanl.gov/abs/cond-mat/9807305.
Storetvedt, K. M. (1997). *Our Evolving Planet*. Bergen, Norway: Alma Matter.
Tassos, S. (2001). Earthquake generation and ophiolite suites in the context of Excess Mass Stress Tectonics (EMST). In *Proceedings of the Global Wrench Tectonics International Workshop,* Fortum Petroleum. Available at: http://www.earthevolution.org/workshop.htm.
Tassos, S. (2002a). Isotropy, volcanism, and heat flow. In *Proceedings of the International Symposium on NCGT*, May 2002, Otero Junior College, La Junta, CO, 231–245.
Tassos, S. (2002b). Anisotropy, spatial and temporal correlation between deep and shallow earthquakes, positive free-air gravity and geoidal anomalies, and the dominance of uplift. In *Proceedings of the International Symposium on NCGT*, May 2002, Otero Junior College, La Junta, CO, 247–277.
Tassos, S. (2002c). The role of micro-fractures in the Excess Mass Stress Tectonics (EMST) Model. *Geology of the Pacific Ocean. 21,* 74–84 (Russian edition).
Tassos, S. (2003). Micro and macro-manifestations of excess mass. In Scalera, G., & Jacob, K.-H. (Eds.), *Why Expanding Earth? A Book in Honour of Ott Christoph Hilgenberg* (pp. 297–331). Instituto Nazionale di Geofisica e Vulcanologia (INGV), Rome, and Technische Universität (TU) Berlin, Rome.
Thordarson, Th., & Self, S. (1993). The Laki (Skaftar Fires) and Grimsvotn eruptions in 1783–1785. *Bulletin of Volcanology, 55,* 233–263.
Uyeda, S. (1986). Facts, ideas and open problems on trench-arc-backarc systems. In Wezel, F. C. (Ed.), *The Origin of Arcs* (pp. 435–460). Elsevier.
Wang, Chi-Yuen. (1978). Some aspects of the Tangshan (China) Earthquake of 1976. In *Chinese Geophysics* (pp. 157–172). American Geophysical Union.
White, R. A. (1999). Precursory deep long-period earthquakes at Mount Pinatubo: Spatio-temporal link to a basalt trigger. Available at: http://pubs.usgs.gov/pinatubo/white/. In Scalera, G., & Jacob, K.-H. (Eds.), *Why Expanding Earth? A Book in Honour of Ott Christoph Hilgenberg* (p. 465). Scalera G. and Jacob K.-H. (eds), Instituto Nazionale di Geofisica e Vulcanologia (INGV), Rome, and Technische Universität (TU) Berlin, Rome.

APPENDIX

Thought Experiment

The attractive gravitational force, F_g, between two masses m_0 and m_1, separated by a distance r, is equal to $F_g = \mathrm{G}m_1m_0/r^2$, where $\mathrm{G} \cong 6.67 \times 10^{-11}\ \mathrm{Nm^2kg^{-2}}$, the gravitational constant. The number of electrons that can

produce an equal repulsive force can be found by using the formula $F_e = q_1 q_0 / 4\pi\varepsilon_0 r^2$, where $\varepsilon_0 \cong 8.854 \times 10^{-12}$ $C^2 m^{-2} N^{-1}$, or the electromagnetic permittivity of "vacuum".

For separation to occur, the gravitational attraction and electrostatic repulsion have to be equal, $F_g = F_e = G m_1 m_0 / r^2 = q_1 q_0 / 4\pi\varepsilon_0 r^2$, then $G m_1 m_0 = q_1 q_0 / 4\pi\varepsilon_0$ and $q_1 q_0 = G m_1 m_0 4\pi\varepsilon_0$. It is important to note that the distance factor is eliminated, and along with it, the arbitrary big-bang singularity contraption, in which at $r = 0$ an infinite amount of energy would be required, or liberated.

For our computations we will take the unit surface area of 1 m^2, at the depth of ~33 km, which is considered as the maximum depth at which microcracks can remain permanently open. Taking a density of about 3000 kg/m^3, a column of 1 m × 1 m × 33 km, has a mass, m_1, or $\sim 10^8$ kg, while the mass, m_0, of a column 1 m × 1 m × 6340 km, with an average density of ~5500 kg/m^3, is $\sim 3.5 \times 10^{10}$ kg.

Considering that $q_1 = q_0$, it follows that $q_1 = q_0 = \sim 0.16$ C. Since the electron charge is $\sim 1.6 \times 10^{-19}$ C, the required amount of "excess" harmonically resonant electrons is in the range of $2 \times 10^{18}/m^2$. Therefore, in the presence of more than 10^{18} "new" electrons/m^2, the rock column at a depth of ~33 km will be separated from its underlying column.